Rapid release of metal salts and nutrients from the 2011 Grímsvötn, Iceland volcanic ash

J. Olsson[1,2*], S. L. S. Stipp[1], K. N. Dalby[1] and S. R. Gislason[2]

[1] Nano-Science Center, Department of Chemistry, University of Copenhagen, Universitetsparken 5, DK-2100 København Ø, Denmark; jolsson@nano.ku.dk; stipp@nano.ku.dk; kdalby@nano.ku.dk

[2] Nordic Volcanological Institute, Institute of Earth Sciences, University of Iceland, Sturlugata 7, 101 Reykjavik, Iceland; sigrg@raunvis.hi.is

* corresponding author

Email: jolsson@nano.ku.dk (J. Olsson)
Telephone number: +45 35 32 02 66
Fax number: +45 35 32 03 22
Postal address: Nano-Science Center, Department of Chemistry, University of Copenhagen, Universitetsparken 5, DK-2100 København Ø, Denmark

Originally submitted to *Geochimica et Cosmochimica Acta*

15 October 2012;

Resubmitted after rewriting and incorporation of the reviewers' comments

29 August 2013

Abstract

On May 21st, 2011, Iceland's most active volcano, Grímsvötn, started its strongest eruption in a century. Grímsvötn produced hundreds of megatonnes of fine basaltic ash, which spread over Iceland, the North Atlantic and Europe. Such fine grained ash can impact human activity and health both with fertilization and with toxicity potential for aquatic environments. The purpose of this study was: (1) to investigate the basic physical and chemical properties of the ash from the 2011 Grímsvötn eruption, (2) to identify surface salts deposited on the ash during the eruption, (3) to identify which elements are released during ash-water interactions and their release rates, (4) to characterize the secondary phases formed during water exposure, and (5) to assess impact of the ash on humans and the environment.

During the eruption, we collected a unique set of pristine ash samples over a range of 50 to 115 km from the source and examined them with X-ray powder diffraction (XRPD), X-ray fluorescence (XRF), surface area analysis (BET), laser absorption, electron microprobe (EMPA), scanning electron microscopy (SEM) and X-ray photoelectron spectroscopy (XPS). The ash could be classified as glassy tholeiitic basalt with <10 mass % crystalline plagioclase ($Al_{1.6}Ca_{0.6}Na_{0.4}Si_{2.4}O_8$) and pyroxene. The particles were small (<125 μm) and elongated with sharp edges. About 50% of the particle mass was fine ash (<63 μm), which could travel long distances, and ~8% was very fine ash (<10 μm), which is harmful if inhaled. The specific surface area of the pristine ash ranged from 0.4 to 0.7 m^2/g. Material taken up on particle surfaces contributed the equivalent of <0.5 nm thick layer, consisting of salts such as $CaSO_4$, Na_2SO_4, NaCl, CaF_2, $CaCl_2$, $MgSO_4$ and $MgCl_2$.

We exposed the pristine ash to ultrapure deionised (MilliQ) water in a single pass, plug, flow through reactor and the effluent was analyzed for 73 elements using inductively coupled plasma sector field mass spectroscopy (ICP-SFMS) and ion chromatography (IC). High release rates of mainly S, Na, Ca, Mg, F and Cl were observed during the first 10 minutes but after 12 hours, the most abundant element released was Si. The effluent was alkaline. Secondary phases of mainly Al and Fe precipitated on the ash surfaces and these were suspected of scavenging As, Ba, Cr, Co, Cu, Ga, Mn, Mo, Ni, P, Te, V and Zn. The maximum total of surface salts containing F, Cl and S, carried by the erupted ash, was 11, 13 and 117 kilotonne. The flux of nutrient and toxic elements from the Grímsvötn ash was low compared with that from other eruptions and would not have been expected to cause poisoning of mammals or aquatic life. The elements most likely to affect sensitive biota were F, Se, Cu and Zn.

Key Words

Tephra deposition, ash dissolution, volcanic ash leachate, ocean fertilization, phreatomagmatic eruption, Vatnajokull, SEM, PHREEQC, XPS.

1. INTRODUCTION

Iceland is one of the most active volcanic regions on Earth, with 30 active volcanic systems that erupt from 20 to 25 times per century and producing more than 5 km^3 of magma (Thordarson and Larsen, 2007; Thordarson and Hoskuldsson, 2008). Many of these volcanos, such as the most productive ones, Grímsvötn and Katla, are covered with glaciers. All subglacial eruption results in volcanic ash production, and sometimes, "Amazonian" size floods to the oceans (Tómasson, 1996; Gislason et al., 2002; Stefansdottir and Gislason, 2005; Thordarson and Hoskuldsson, 2008).

These eruptions and floods are important, (1) because they can provide rate determining nutrients for the growth of phytoplankton in the surface waters of the North Atlantic, one of the largest atmospheric CO_2 sinks on Earth (Frogner et al., 2001; Takahashi et al., 2009); (2) because of its location and prevailing winds, volcanic ash from Icelandic volcanoes can cause air traffic disturbance over western Europe for days (EC, 2010; EC, 2011; Gislason et al., 2011b); and (3) because these eruptions can cause local and global pollution of the atmosphere and surface waters (Grattan and Gilbertson, 1994; Thordarson and Self, 2003; Flaathen and Gislason, 2007; Ayris and Delmelle, 2012b).

The Grímsvötn volcano is located within the Vatnajökull Glacier in southeastern Iceland (Fig. 1), which is the largest glacier outside the polar regions. Grímsvötn is the second most productive Icelandic volcano, with 60 known eruptions since the beginning of the 12^{th} century (Thordarson and Larsen, 2007). The enormous Laki eruption 1783-1784 came from the Grímsvötn volcanic system and produced 14.7 km^3 of lava and about 0.4 km^3 (DRE) of tephra. It released about 120 Mt of SO_2 into the atmosphere, producing an aerosol cloud that covered the northern quarter of the globe. This resulted in significant environment and climatic consequences (Thordarson and Self, 1996; Thordarson and Self, 2003; Chenet et al., 2005; Oman et al., 2006). The sulfur dioxide emission changed global climate, resulting in "no summers" in Europe. The resulting disturbance in crops caused mass suffering and might have been the trigger for the French revolt in 1785 (Grattan and Brayshay, 1995; Bojanowski, 2011).

The Grímsvötn volcano began to erupt during the evening of May 21, 2011. The eruption was the strongest in more than a century and it continued until May 28, 2011. Hot magma interacted with melt water and steam, causing a highly explosive phreatomagmatic eruption, which produced very fine ash particles. Fine ash can be suspended in air for

days and be dispersed over large distances (Bursik et al., 1992; Durant et al., 2010). The ash plume of Grímsvötn rose to 20 km and ~350 megatonnes of volcanic ash were carried over Iceland, the North Atlantic and Europe (Gudmundsson et al., 2012a; Tesche et al., 2012; Lieke et al., 2013).

Volcanic ash is generally produced by the expansion of magmatic gases. As magma ascends to the Earth's surface and pressure decreases, gases become supersaturated; bubbles nucleate and grow within the magma. The lower viscosity of silica poor magmas, such as basalt, allows gas bubbles to rise rapidly to the surface, in contrast with more viscous, silica rich magmas, such as andesite-rhyolite (Cashman et al., 2000). Eruptions of basaltic magma are therefore most often gentle and effusive. The viscosity of ascending magma increases as the magma degasses, which retards growth and causes overpressurization of the bubbles. When a threshold gas volume of at least 60% of the total gas and magma is reached, the overpressured bubbles burst into fragments and ash is produced. (Sparks, 1978; Cashman et al., 2000; Rust and Cashman, 2011). If magma of any composition, basalt to rhyolite, comes into contact with water, such as the water melted from an overlying glacier, it fragments, resulting in a phreatomagmatic eruption.

Magmatic volatiles are scavenged by ash particles during their transport in the volcanic plume. The gases are taken up by gas-particle and liquid-particle interactions (Taylor and Stoiber, 1973; Oskarsson, 1980; Delmelle et al., 2007; Martin et al., 2012). As the erupted plume cools, the volatiles condense onto the ash particle surfaces or as "single droplets" (Rose, 1977; Rose et al., 1980). The particles react with air and water vapor and the condensed gases form sulfuric and halogen acids, which promote dissolution of the ash particle surfaces during transport. Cations are leached by the acids and these precipitate with the gas condensates as a thin coating or discrete secondary phases on the ash particle surfaces (Rose, 1977; Oskarsson, 1980; Africano and Bernard, 2000; Delmelle et al., 2007; Gislason et al., 2011b). Some of these surface deposits dissolve rapidly when the particles come into contact with water. Depending on their composition, they can fertilize or poison aquatic environments.

During the last decades, dozens of leachate studies have been conducted on volcanic ash from all over the world and the presence of more than 50 elements and some isotopes have been detected (Witham et al., 2005; Alfredsson et al., 2012). The geochemical composition of ash and leachate have been used to demonstrate that single volcanic eruptions have the potential to significantly increase the local concentration of metals in the surface ocean waters (Frogner et al., 2001). Studies of Pacific Ocean sediments have shown that, on time scales of millenia, airborne volcanic ash has been responsible for a flux of Fe that is comparable to that of mineral dust (Mahowald et al., 2005; Olgun et al., 2011).

In this study, we report the basic properties of a unique set of pristine (dry, fresh) ash samples, collected during the 2011 Grímsvötn eruption. Parameters derived include surface area, grain size distribution, bulk and surface composition. The Grímsvötn ash samples were exposed to water in single pass, plug, flow through reactors. We checked for the presence of 74 different elements from the ash. The purpose of the study was: (1) to determine physical and chemical characteristics of the Grímsvötn ash, (2) to gain new insight into the element release rate during the first minutes of exposure to water, as well as after several weeks, (3) to characterize the secondary phases formed on the ash surface during water exposure, (4) to identify which salts deposited on the ash surfaces during the eruption and (5) to discuss potential environmental impacts of the elements released from phreatomagmatic ashes, such as that of Grímsvötn 2011.

2. MATERIAL AND METHODS

2.1. Ash sample collection

The Grímsvötn ash was sampled on May 22, 2011, from 16:05 to 19:30 GMT, after most of the total mass of the erupted material had already been ejected[1] (Petersen et al., 2012) (Table 1). The wind carried the ash mainly in a northerly/northeasterly direction (Petersen et al. 2012). Eight pristine ash samples were collected across the major axis of the fallout, along the main road in southeastern Iceland, 50-115 km south/southwest of the summit (Fig. 1). The samples integrate the main fallout during the first 21 to 24 hours of the eruption, when the effusive rate was highest and the plume rose to more than 10 km (Petersen et al., 2012). Collection of these samples could have missed volcanic ash that was produced during a minor effusive phase and transported less than 50 km from the eruption site. The ash was dark grey, soft and powdery in the field. For sampling, we used a plexiglass spatula to shovel several kilos of ash into heavy walled polyethylene bags. For long term storage, samples were kept in air tight glass containers. The relative humidity during collection ranged from 44 to 73%. The weather was calm, with no rain (Table 1). Ash is hygroscopic and with time it equilibrates with its physicochemical surroundings so aging could affect the potential release of elements from the ash (Jones and Gislason, 2008; Olgun et al., 2011), e.g. the morphology of fresh olivine surfaces changes within hours of exposure to air (Olsson et al., 2012) and calcite has been shown to recrystallise simply in the water layer adsorbed from the humidity of air (Stipp et al., 1996). Therefore, our samples were analyzed very soon after collection, in some case within days. An adsorbed water layer on the surface of ash particles could certainly dissolved deposited salts, allow reactions and the formation of secondary phases that were not a direct result of the eruption. It was therefore crucial for our leachate study to

[1] Magnus T. Gudmundsson, Institute of Earth Sciences, University of Iceland, personal communication, July 4, 2012.

use samples that were absolutely fresh, pristine and unhydrated, i.e. ash that had not been in contact with water during or following deposition. Interaction with water vapor from phreatomagmatic activity, the volcanic plume and the atmosphere, however, could have impacted the water content on the ash surface (Delmelle et al., 2005; Lathem et al., 2011).

2.2. Experimental set up

Similar to previous ash-leachate studies, the experiments were conducted in single pass, plug, flow through Teflon reactors (Frogner et al., 2001; Jones and Gislason, 2008). The reactors had an inner diameter of 10 mm and were approximately 18.2 cm long; with cap screws the total length was 20 cm. The influent passed through a 125 µm nylon sieve and the effluent passed through another nylon sieve and two additional 0.2 µm cellulose acetate membrane filters (Fig. 2). At a flow rate of 60 ± 5 mL/h, MilliQ water was continuously pumped through the flow reactor, which contained approximately 12 g of fresh ash. The overall water-ash contact time was 11 ± 2 minutes. With a 3 way valve, the effluent was either directed to the bottom of a 20 mL plastic beaker for real time pH measurement or collected as samples. The liquid samples were analyzed with ion chromatography (IC), inductively coupled plasma optical emission spectrometry (ICP-OES) and in some cases, with inductively coupled plasma sector field mass spectroscopy (ICP-SFMS). The sample effluent tube could be connected directly to the IC for instant analysis to avoid sample-air contact. Injecting samples directly into the IC gave the option to quantitatively determine sulfur species that would have oxidized rapidly in air.

2.3 Characterization techniques and parameters

For identifying the major crystal phases of the ash, X-ray powder diffraction (XRPD) was used. Patterns were collected in a STOE STADIP, 61146 diffractometer equipped with a Cu-Kα radiation source and a germanium monochromator. Scans were taken from 2° to 60°, using 2θ steps of 0.1° and a 150 s counting time per step. The XRPD patterns were compared with the powder diffraction standards in the PDF-2 file for mineral identification (International Center for Diffraction Data, 1995). The major oxides and the loss on ignition (LOI) of the bulk ash were determined by $LiBO_2$ fusion followed by X-ray fluorescence (XRF) on an Axios-Minerals spectrometer at Acme Analytical Laboratories, Vancouver. A complete list of the analyzed elements can be found in the Electronic Annex EA-1.

X-ray photoelectron spectroscopy (XPS) was used to investigate the chemical composition and electronic states of the top atomic layers of the ash particles. When

analyzing the top few atomic layers only, clean tools and working conditions are absolutely necessary to minimize the accumulation of air borne carbon contamination called adventitious carbon (Stipp and Hochella, 1991). Lateral spot size is about 500 µm but vertical information depth with XPS is in general ~10 nm or less making it extremely surface sensitive. All XPS analyses were conducted with a Kratos AXIS Ultra instrument using a monochromatised $Al_{K\alpha}$ X-ray anode and slow electron charge compensation. The survey spectra were made with pass energy of 160 eV and with a 0.3 eV step size and all narrow scans with pass energy at 10 eV and 0.1 eV step size. The binding energy resolution is about 0.35 eV at 10 eV pass energy (Nesbitt et al., 2004). The XPS data were processed using the CasaXPS software after Shirley background treatment (Shirley, 1972). Spectra were calibrated by assigning the adventitious C 1s peak to be 285.0 eV.

The BET (Brunauer et al., 1938) surface area was determined using N_2 adsorption by the 5 point method with Tristar 3000 and Quantachrome Nova 2200 instruments. Before BET analysis, the samples were heated to 150 ºC in vacuum. Supplementary experiments show that surface area obtained for samples heated between 60-200 ºC vary within 10% uncertainty (Electronic Annex EA-2). Particle size and particle size distribution were determined using the >125 µm fraction collected by dry sieving. The size distribution for the <125 µm fraction was determined by laser absorption in a dry dispersion, created using vibration, differential pressure and air. The detection limit was 1.8 µm.

Polished sections for electron microprobe analysis (EMPA) were prepared by standard procedure and coated with about 10 nm of carbon using a JEOL (JEC 560) Auto Carbon Coater. The quantitative chemical microprobe analysis was conducted with a JEOL-microprobe (JXA-8200) operating at an accelerating voltage of 15 kV and a beam current of 15 nA. The elements were analyzed using their Kα spectrum lines and the standards were natural and synthetic silicates and oxides. The counting time was 10 s. Scanning electron microscopy (SEM) images were collected with an FEI Quanta FEG 3D, running in secondary electron mode at 2.0 kV. SEM samples were coated with a few nanometers of Cr.

The chemical components of the plug flow reactor effluents were analyzed with ion chromatography (IC) and inductively coupled plasma optical emission spectrometry (ICP-OES) at the Institute of Earth Sciences, University of Iceland, and standardized with in house multi element standards. The in house standards are regularly tested by analyzing the Standard Canadian River Waters (SLRS-4) and single element international standards (SPEX). The F^-, Cl^-, NO_3^-, SO_4^{2-}, SO_3^{2-} and $S_2O_3^{2-}$ concentrations were determined by IC and the rest with ICP-OES. Comparison of IC measurements for direct injected samples with samples that were stored in vials for 24 hours before analysis showed minimal oxidation of thiosulfate (data not included). All samples analyzed for $S_2O_3^{2-}$ were measured within 24 hours. Selected samples were analyzed at Analytica-SGAB, Luleå, with inductively coupled plasma sector field mass spectroscopy (ICP-

SFMS) for 71 elements. We analysed quantitively: Al, As, B, Ba, Be, Ca, Cd, Ce, Co, Cr, Cs, Cu, Dy, Er, Eu, Fe, Gd, Hg, Ho, K, La, Li, Lu, Mg, Mn, Mo, Na, Nd, Ni, P, Pb, Pr, S, Si, Sm, Sn, Sr, Tb, Ti, Tm, U, V, Yb, and Zn; the rest were analysed semiquantitatively (Bayon et al., 1998). Samples for ICP-OES and ICP-SFMS analysis were acidified immediately after sampling with concentrated suprapure HNO_3.

Generally, there was less than 15% difference between corresponding aqueous element concentrations measured with the two different ICP methods. Exceptions were concentrations of Al, Mn and S (total), which in some cases resulted in differences of as much as 30%. Concentrations, uncertainties and detection limits of all released elements can be found in the Electronic Annex EA-3. We measured pH using a glass combination electrode at laboratory temperatures; the pH meter was calibrated with certified pH buffers from Oakton.

There was a very small volume of sample effluent from the initial part of the experiment and we needed all we had for the element determinations so we made a parallel leaching experiment for collecting effluent for measuring pH during the first 24 hours. The cation and anion charge balance was generally within 10% except for samples collected in the time interval 20-150 minutes. The rapid pH increase during this time caused underestimation of the OH^- ion activity because the effluent volume for the pH measurement was 20 mL while the volume collected for chemical analysis in the time interval 0-150 minutes was 3-15 mL. The difference in volume returned a lower time resolution for the pH values than for the chemical analyses, which resulted in a small pH offset error for the periods where pH changed rapidly. The error was easily corrected by forcing a charge balance using the PHREEQC computer code (Parkhurst and Appelo, 1999). PHREEQC is an aqueous modelling program designed to perform a wide range of geochemical calculations in combination with a thermodynamic database. In this work, the charge balance, total alkalinity, activity and the saturation state were all determined using PHREEQC with the MINTEQ.v4 database and data added for forsterite, fayalite, $Fo_{80}Fa_{20}$, $Fo_{43}Fa_{57}$, enstatite, ferrosilite, diopside, hedenbergite, orthopyroxene, clinopyroxene, anortite, albite, $An_{70}Ab_{30}$, $An_{29}Ab_{71}$ and basaltic glass, from Eiríksdóttir et al. (2013). To estimate alkalinity, the amount of HCl needed to decrease pH of the reactor effluent to pH 5.9 was determined with PHREEQC. All modelled solutions were set to be initially in equilibrium with atmospheric partial pressures for oxygen and CO_2.

3. CALCULATIONS

The element release rates were determined using the expression (Berner, 1995):

$$R = \frac{c \cdot Q}{s_{BET} \cdot m}, \qquad (1)$$

where C represents the element concentration, Q refers to the liquid flow rate, s_{BET} denotes the measured BET specific surface area and m represents the mass of the ash sample. The release rates in Figure 4 were not normalized with respect to the BET surface area but rather, simply the mass of ash. This allows direct comparison of release rates from previous plug flow reactor studies (Frogner et al., 2001; Jones and Gislason, 2008).

The roughness factor of a surface is defined as s_{BET}/s_{geo}, where s_{BET} represents the measured BET surface area and s_{geo}, the geometric specific surface area (Jaycock and Parfitt, 1981). The geometric specific surface area was estimated assuming that the ash particles were perfectly smooth spheres or cubes (Tester et al., 1994):

$$s_{geo} = \frac{A}{V \cdot \rho} = \frac{6}{\rho \cdot d_{eff}}, \qquad (2)$$

where A and V denote the surface area and the volume of a sphere or a cube. The glass density, ρ, was set to 3.0 g/cm^3 (Wolff-Boenisch et al., 2004b) and the effective particle diameter, d_{eff}, was used directly from the grain size distribution (Electronic Annex EA-4).

Derived values of the Si release rate (CSiR), stemming from bulk dissolution of basaltic glass at 25 °C, were based on the far from equilibrium dissolution rate of basaltic glass ($r_{+,geo}$) at variable solution composition:

$$CSiR = r_{+,geo} \cdot s_{geo} = A_A \, exp^{-\left(\frac{E_a}{RT}\right)} \left(\frac{a_{H^+}^3}{a_{Al^{3+}}}\right)^{1/3} \cdot s_{geo}, \qquad (3)$$

where A_A is a constant, $10^{-5.6}$ (mol of Si)/cm^2/s; E_a represents the activation energy, 25.5 kJ/mol; R is the gas constant and T represents the absolute temperature (Gislason and Oelkers, 2003). The activities of H^+ and Al^{3+} were determined from the measured solution compositions using the PHREEQC computer code.

4. RESULTS

4.1. General properties of the Grímsvötn ash

Based on its chemical composition, the Grímsvötn ash was tholeiitic basalt and mostly glass (Table 2). The EMPA and X-ray powder diffraction (XRPD) analysis demonstrated that the amorphous glass matrix also contained 10> mass % crystalline plagioclase ($Al_{1.6}Ca_{0.6}Na_{0.4}Si_{2.4}O_8$), pyroxene and trace amounts of diopside and iron oxides (Fig. 3, XRPD data not shown). The XPS analysis, which collected data from the top few nanometers of the ash surface, show in order of abundance, O, Si, Al, Fe, Ca, Na, Mg, S, Ti and traces of F and Cl (Table 2 and Electronic Annex EA-5).

Ash samples, 1, 6, 7, and 8 were chosen for extensive analysis by a variety of techniques. These represent the samples taken closest to and furthest away from the eruption site, as well as samples where the ash fallout was greatest along the sampling path (Table 1 and Fig. 1). The EMPA and SEM images show elongated particles with sharp edges (Fig. 3a and b). They were <200 µm in diameter and smaller particles were often observed attached to larger grains. Particle size distribution data show that the ash was mostly fine grained with a size distribution peak around 60 µm (Fig. 3c). About 50-65% of the particulate mass was classified as fine ash, i.e. diameter <63 µm (Electronic Annex EA-4). Fine ash can remain suspended in air for days, travelling far (Bursik et al., 1992; Delmelle et al., 2005). Particles in the size range that constitute increased risk when inhaled, i.e. <10 µm, were present as at least 8-10% of the mass, not counting the material that adhered to the larger grains (Horwell and Baxter, 2006). The measured BET surface area for the ash samples ranged from 0.44-0.63 m^2/g. Comparison of the measured BET surface area with calculated geometric surface area revealed surface roughness factors of 5 to 10 for the Grímsvötn ash.

4.2. Release of elements from the Grímsvötn ash

Plug flow experiments were conducted to mimic the element release from the Grímsvötn ash into water in natural systems. Water was continuously pumped through the reactor filled with ash and a series of water effluent samples was collected over time (Section 2.2 and Fig. 2). High time resolution, i.e. frequent sampling, is required to observe the elemental release from surface deposits on ash, because some of these dissolve nearly instantaneous (Gislason et al., 2011b). Therefore, each sample collected during the first two hours was just enough for the chemical analysis. Of the 74 elements analyzed with ICP-SFMS and IC, a total of 51 elements were detected (Electronic Annex EA-3 and EA-6).

The element release rate, including some rare earth elements (REE), generally showed a fast decay with time, decreasing by more than an order of magnitude within the first 10 minutes (Fig. 4 and Electronic Annex EA-7). In the beginning of the experiment, release of S, Na, Ca, Mg, F and Cl dominated but after 12 hours, the most abundant element released was Si (Fig. 4). The IC measurements demonstrated that the sulfur species were mainly SO_4^{2-} but SO_3^{2-} and $S_2O_3^{2-}$ were also detected. The SO_3^{2-} concentration was near the detection limit so it was not quantified. Thiosulfate ($S_2O_3^{2-}$) has been found in flood waters associated with volcanic eruptions under glaciers in Iceland (Gislason et al., 2002). The release rate of all the measured anions decreased several orders of magnitude to under the quantification limit within the first 24 hours.

The pattern of pH change, shown in Figure 4b, suggests three main stages. The first is a slow, steady increase from pH 7.3, measured after 4 minutes, to pH 7.7, after 25 minutes. The second stage is a fast increase, reaching a pH maximum at 9.7 after about 160 minutes. The final stage is a steady decrease to pH 7.7 over 15 days (Fig. 4b). The pH change with time parallels and influences the release rate of several elements. For example, after an initial decline, the release rate of Al, Cr, Co, Fe, Ni, Cu, Zn, P, V and Mo, increased during the period from 50 to 110 minutes, in parallel with a rise in pH (Fig. 4). Other elements with similar behavior were As, Ba, Ga and Te (Electronic Annex EA-7).

The release rates of the selected nutrients, Fe, Mo, NO_3, P and V are shown in Figure 4d. At first, the NO_3 release rate is highest and decreases most rapidly with time. After 30 minutes, P release dominates, followed by V. The P and V release rates increase with time, in parallel with a rapid rise in pH (Figs. 4b and d). The Fe release rate was surprisingly low, about 1 nmol/g/h.

4.3. PHREEQC modelling

The PHREEQC model was used to determine the total alkalinity and the saturation state of solid phases in the effluent samples (Fig. 5). Alkalinity was 0.01 mEq/L initially. It increased slowly during the first 10 minutes, then increased dramatically to 0.2 mEq/L at 20 minutes (Fig. 5a), remained stable until 50 minutes, then gradually decreased to 0.01 mEq/L over the next 15 days. The saturation states were used to determine secondary phases that could precipitate. These were: birnessite (MnO_2), ferrihydrite ($Fe(OH)_3$), gibbsite (α-$Al(OH)_3$), goethite (FeOOH), hydroxylapatite ($Ca_5(PO_4)_3OH$), kaolinite ($Al_2Si_2O_5(OH)_4$) and manganite (MnOOH) (Fig. 5b). Birnessite, goethite and manganite were generally the most supersaturated phases. During the time interval 10-200 minutes, when pH was most alkaline, the Mn, Fe and Al phase supersaturation decreased and the saturation of hydroxylapatite dominated. Several other phases were supersaturated, such as barium arsenate ($Ba_3(AsO_4)_2$), barite ($BaSO_4$), boehmite (γ-AlOOH), cuprousferrite ($CuFeO_2$), diaspore (α-AlOOH), fluorite (CaF_2), hausmannite (Mn_3O_4), hematite (Fe_2O_3) and lepidocrocite (FeOOH) but these minerals probably could not precipitate within the time frame of the experiments.

5. DISCUSSION

5.1. Examination of the surface deposits on the Grímsvötn ash

In general, the amount of surface salts on volcanic ash is limited, probably less than the equivalent of a nanometer thick coating if it was distributed evenly over the ash surface. This estimate assumes the surface area determined using the BET method (Gislason et al., 2011b). Surface material was patchy, not evenly distributed on Eyjafjallajökull ash surfaces (Bagnato et al., 2013). The tiny amount complicates direct analysis and thereby also the correct identification of the surface salts. Stoichiometric estimates of leached elements, together with XPS analyses, have previously been applied for indirect identification of salts on ash (Delmelle et al., 2007; Gislason et al., 2011b; Durant et al., 2012). We interpreted XPS binding energies to obtain information about the electronic state and to identify the surface components. The binding energies of Si (2p) at 102.7 eV, Mg (2p) at 50.2 eV, Ca ($2p_{3/2}$) at 347.9 eV, and Na (1s) at 1072.6 eV are indicative of silicate phases (Moulder et al., 1995; Zakaznova-Herzog et al., 2005; Zakaznova-Herzog et al., 2006; Zakaznova-Herzog et al., 2008). The majority of these elements is probably bound in the glass, plagioclase and pyroxene phases. Direct identification of the soluble surface salts is difficult because of the limited amount and the greater contribution from the bulk ash. However, the detection of fluorine and chlorine, along with the S (2p) binding energy at 169.5 eV, indicates the presence of fluoride, chloride and sulfate salts (Table 2 and Electronic Annex EA-5).

To identify the surface deposits on pristine ash, the surface composition, measured with XPS, was compared to bulk composition, measured with XRF. The data showed surface enrichment of Si, Al, Na and S and depletion in Fe, Ca, Mg, K and Ti, relative to the bulk composition of the glass (Fig. 6, Table 2). Dissolution of glass is known to selectively remove mono- and divalent cations from the surfaces and leave behind a framework enriched in Si, Al and Fe (Berger et al., 1987; Oelkers and Gislason, 2001). This suggests some dissolution of the ash already before fallout but some Na and S salts could have condensed from the plume. Similar results were obtained in a comprehensive XPS study of several different ash samples by Delmelle et al. (2007). They noticed a systematic surface depletion of Fe, Ca, Mg, K and Na and higher concentrations of Si, Al, F, Cl and S relative to the ash bulk and explained this by in-plume dissolution. Other studies showed ash surfaces with increased amounts of Al, Ca, Fe and Na for the Chaitén volcano, Chile and for the 2010 eruption of Eyjafjallajökull, Iceland, higher Si, Al and Mg (Gislason et al., 2011b; Durant et al., 2012).

For the Grímsvötn ash, the tiny amount of surface deposits was barely detectable even with XPS. The initial leachate waters, however, contained substantially increased concentrations of Na, Ca, Mg, Cl, F and especially S relative to Si (Fig. 4 and Electronic Annex EA-3). The data from our leachate experiments suggested that dissolution of non-silicate phases dominated during the first minutes of ash-water interactions. The charge balance error is less than 5% so it is possible that the most concentrated elements, i.e. S, Na, Ca, Mg, Cl and F (in order), of the first leachate samples originate from surface salts.

Simple stoichiometric estimates support the presence of $CaSO_4$ and Na_2SO_4, which have also been observed by others (de Hoog et al., 2001; Delmelle et al., 2007; Durant et al., 2012). Other candidates are NaCl, CaF_2, $CaCl_2$, $MgSO_4$ and $MgCl_2$, which are all typical surface deposits for pristine volcanic ash (Naughton et al., 1974; Rose, 1977; Oskarsson, 1980; Rose et al., 1980; Taylor and Lichte, 1980; Allard et al., 2000; de Hoog et al., 2001; Cronin and Sharp, 2002; de Moor et al., 2005; Le Blond et al., 2010; Bagnato et al., 2013). A simple estimate from the bulk dissolved concentration data suggests that the total mass of the salts is ~0.8‰ of the bulk mass of the sample. These salts were probably both distributed as small grains and surface coatings on the surface (Gislason et al., 2011b; Bagnato et al., 2013). If the salts were evenly distributed over the surface, where surface area is determined using the BET method, and not hydrated, their average thickness would be ~0.5 nm. This is the same thickness (0.6 nm) as was determined for the phreatomagmatic explosive ash of Eyjafjallajökull (Gislason et al., 2011b).

5.2. Dissolution of the surface deposits on the Grímsvötn ash

During exposure to ultrapure deionised (MilliQ) water, the Grímsvötn ash released no less than 51 different elements, including some rare earth elements (REE) (Electronic Annex EA-6 and EA-7). Rare earth and refractory trace elements are known to be present as volatiles in volcanic plumes so it is likely that these accumulated on the ash surface during eruption (Moune et al., 2010; Mather et al., 2012). The release rates of a wide range of elements decreased rapidly with time, consistent with similar plug flow reactor studies conducted on volcanic ash (Frogner et al., 2001; Jones and Gislason, 2008; Alfredsson et al., 2011). The most soluble surface deposits dissolved first. During the first 10 minutes, the highest release was observed simultaneously with relatively low net proton consumption, as is reflected in the development of pH and alkalinity in Figures 4b and 5a. Either the protons released from potential proton salts were consumed by *in situ* silicate dissolution or the initial dissolution stage neither released nor required protons, i.e. simple dissolution of metal salts.

Dissolution of metal salts, such as $CaSO_4$, Na_2SO_4, NaCl, CaF_2, $CaCl_2$, $MgSO_4$ and $MgCl_2$, neither consumes nor produces protons. However, an increase in alkalinity was observed after about 10 minutes (Fig. 5a). Dissolution of silicate materials, such as basaltic glass, plagioclase and pyroxene, builds up alkalinity by consuming protons, releasing cations and increasing the relative amount of Si compared with other leachates, as seen in Figures 4a, b and 5a (Gislason and Eugster, 1987; Oelkers and Gislason, 2001). We propose that the initial high release rate of Ca, Cl, F, Mg, Na and S relative to Si represents a combination of dissolution of surface deposits and preferential leaching of these ions from the bulk ash. Over time, dissolution of the bulk ash became the dominate release reaction. This matches the continuous increase of released Si relative to the other

leachates (Fig. 4). Corners, edges and small particles of the bulk glass dissolve fastest (Oelkers and Gislason, 2001) and together with preferential leaching of cations, this forces a rapid increase in pH and alkalinity of the effluent waters. As the easy accessible cations are leached from the bulk and the higher free energy corners, edges and small particles are consumed, dissolution rate decreases, resulting in decreased proton consumption. Alkalinity reached its maximum after about 50 minutes and decreased thereafter because of diminishing proton consumption and precipitation of secondary minerals.

Dissolution rate for bulk volcanic glass is controlled by temperature, saturation state and solution composition through the H^+ and Al^{3+} activity as shown in Equation 3 (Gislason and Oelkers, 2003). The formation of Al-C_2O_4, Al-F and Al-SO_4 complexes affects glass dissolution only in acidic to neutral conditions (Oelkers and Gislason, 2001; Wolff-Boenisch et al., 2004a; Flaathen et al., 2010). The Si release rates (CSiR), generated with Equation 3, can be directly compared with measured rates (Fig. 4a). For the first 10 minutes, the observed rate was faster than the estimate. Only after about 30 minutes did the calculated and observed rates match. After 35 minutes, the estimate was higher than the observed rate and the gap between the two continued to increase over time. This increasing difference most likely results from precipitation of secondary silicates and Al, Fe and Ti phases. Additional evidence for this interpretation is that element release was never stoichiometric with respect to the bulk ash, not even after 15 days.

5.3. Formation and dissolution of secondary phases

Fractions of element concentrations originating from the dissolved surface deposits might not be measured in the effluent water of the plug flow reactor because they could immediately precipitate or coprecipitate as less soluble new phases, partly on the ash surfaces. The surface composition of the ash changed during the course of the plug flow reactor experiments. The relative concentration of Na, S, Ca, Mg, F and Cl had decreased, whereas Al, Fe and Ti had increased after 15 days of exposure to pure water (Fig. 6, Table 2). A slightly higher Si ratio was observed on ash surfaces exposed to water for 15 days than on fresh surfaces but the surface Si concentration decreased again for ash exposed to water for 4 weeks (Electronic Annex EA-5). Our PHREEQC calculations show that the effluent was supersaturated with respect to several Si, Al, Fe and Mn phases (Section 4.3 and Fig. 5). The surface enrichment of Fe and Al indicated the formation of secondary phases during water exposure.

Al, Fe and Mn readily form pH dependent precipitants, such as oxyhydroxides, hydroxides and oxides. These precipitants also can absorb a wide range of dissolved components (e.g. Kinniburgh et al. (1975); Kinniburgh et al. (1976); McKenzie (1980);

Okazaki et al. (1986); Pavlova and Sigg (1988); Sposito (1995); Stumm and Morgan (1996); Lee et al. (2002); Cornell and Schwertmann (2003)). Important parameters controlling these reactions include pH, temperature and ionic strength (Sposito, 1995; Lee et al., 2002; Cornell and Schwertmann, 2003; Pentecost, 2005). Thus, the chemical release from ash depends on the local physicochemical conditions. Results from our plug flow reactor experiments show excess release of Al analogous to an increase in pH and decrease in saturation state of the aluminium phases, gibbsite and kaolinite (Fig. 4 and Fig. 5b). We propose that several elements are scavenged in secondary phases that form instantly on the surface of the ash particles on contact with water. The increase in pH during the time interval from 30 to 200 minutes mobilized increased amounts of Al, As, Ba, Cr, Co, Cu, Fe, Ga, Mo, Ni, P, Te, V and Zn, which probably had been caught in soluble aluminium and iron phases, such as those proposed in Figure 5b. An abrupt dissolution of these scavenging phases and release of unwanted elements into surface waters would probably only happen during extreme environmental conditions (e.g. pH > 9). An example of a exposed water body is the groundwater fed Lake Mývatn, North Iceland, where during the summer, pH rises above 10 (Thorbergsdottir and Gislason, 2004).

A similar study conducted on ash from Hekla, Iceland suggested that secondary mineral formation had a dominant effect on the release rates of some elements (Jones and Gislason, 2008). The formation of secondary phases and surface recrystallization on silicate minerals can effect dissolution kinetics (Schott and Berner, 1983; Wogelius and Walther, 1992; Béarat et al., 2006) but a recent study demonstrated that calcite precipitation does not affect the overall dissolution rate for basaltic glass (Stockmann et al., 2011). Secondary phases formed on the ash particle surface during water contact can sequester trace elements, thus inhibiting their release. Understanding the pH sensitive capture and release processes of the secondary phases is important for assessing the environmental impact of ash fall. Toxic elements can accumulate in precipitating secondary phases in surface waters contaminated by ash. A simple change in the water chemistry, such as pH, temperature, ionic strength or elements present, can redissolve the precipitates and trigger a delayed pulse of toxic element release into the aquatic environment.

5.4. Element fluxes

We define the element flux as the total amount of an element released over time from one gram of Grímsvötn ash. Fluxes are useful to estimate the fertilization and pollution potential of released elements, or for calculating the total amount of volatiles sorbed by the ash (Frogner et al., 2001; Jones and Gislason, 2008). The element release rate, and thereby the flux, depends on physicochemical factors such as temperature, pH, dissolved

constitutes, ionic strength, water turbulence etc., in addition to the ash to water ratio (Witham et al., 2005). Therefore care must be taken before adapting these numbers directly to other systems. The pH in our experiments was alkaline. This contrasts with effluent from other plug flow reactor studies conducted on ash from all over the world (Frogner et al., 2001; Jones and Gislason, 2008) but resemble the phreatomagmatic ash of the Eyjafjallajökull 2010 eruption (Alfredsson et al., 2011). The fluxes are probably related directly to the composition, thus the acidity level, of the ash. A complete list of all the estimated fluxes from the Grímsvötn ash is presented in the Electronic Annex EA-6.

5.4.1. Fluoride, chloride and sulfur released by volcanic ash

The volatiles released from volcanic events have an impact on the natural environment (Gerlach and Graeber, 1985; Robock, 2000; de Hoog et al., 2001). Acidic aerosols form in the atmosphere when volcanic gases react with water, which reflect or absorb solar radiation, affecting temperature and producing acid rain. Furthermore, knowledge of the total volatile budget is important for estimating plume composition or for discussing magmatic processes, such as fragmentation and degassing (Gerlach and Graeber, 1985; Cashman et al., 2000; de Hoog et al., 2001; de Moor et al., 2005). Considerable amounts of volatiles adsorb on volcanic ash, e.g. S in quantities as high as 25% (Taylor and Stoiber, 1973; Rose, 1977; de Hoog et al., 2001; de Moor et al., 2005). These scavenged gases must be accounted for when the total mass of released volatiles is estimated.

During the 15 days of our experiments, the flux of material released from the Grímsvötn ash was 0.85 µmol/g for F, 0.54 µmol/g for Cl and 5.3 µmol/g for S (Electronic Annex EA-6). In comparison with the ash samples studied previously by Jones and Gislason (2008) only Galeras, Columbia 2005 and Hekla, Iceland 2000 released significantly higher amounts of surface F and S. In comparison with the ash samples from other sites around the world studied by Jones and Gislason (2008), the average specific sulfur release rate for the first 8 hours from the Grímsvötn 2011 ash was lower than that released from the Galeras, Colombia ash from November 2005 but it was similar to ash from Montserrat, United Kingdom in 2003; Santiaguito, Guatemala in 1998 and Hekla, Iceland in 2000. It should be noted that the release rates were normalized by mass and not by specific surface area. The Cl release from the Grímsvötn 2011 ash was exceptionally low, compared with the more silica rich ash of the other locations. It is likely that the composition of the magma and the phreatomagmatic character, i.e. the ash-melt water interaction, considerably limited the quantity of the more water soluble volatiles (e.g. HCl) from the vapor phase, condensing on the ash particles.

In a recent work by Bagnato et al. (2013), a set of leaching experiments was carried out on fresh ash from the Eyjafjallajökull eruption. Their results show a low mean release of

F and S and *"extremely"* low Cl release from ash collected during the benmoreite (relative low SiO_2 content of the erupted groundmass glass) and phreatomagmatic stages of the eruption (Gudmundsson et al., 2012b). A change of the eruption character to an explosive and more silica rich stage coincided with higher amounts F, Cl and S on the ash surfaces. The mean flux per gram of ash increased for F from 3.3 to 13 µmol/g, for Cl from 1.8 to 3.7 µmol/g, and for S from 0.50 µmol/g to 2.0 µmol/g. Bagnato et al. (2013) argued that the ash from the first two stages of the eruption might not have been pristine and therefore the amount of surface deposits might have been lower. The authors also noted that an even lower quantity of water soluble surface deposits was observed in a similar study done on pristine ash from the phreatomagmatic stages of the Eyjafjallajökull eruption (Gislason et al., 2011b). Gislason and coworkers explained that the ash-melt water interaction had limited the amount of the more water soluble volatiles available to condense on the ash particles because of washout by the melt water.

The total volume of ash produced during the Grímsvötn 2011 eruption was estimated to 0.25 km^3 of dense rock equivalent, corresponding to $6.9 \bullet 10^{14}$ g of ash (Gudmundsson et al., 2012a). Assuming that our samples represent a reasonable average of all ash ejected from Grímsvötn, the total F, Cl and S released as ash surface deposits is estimated to be 11, 13 and 117 kilotonne. The flood waters from the 1996 subglacial eruption of Gjálp, near Grímsvötn carried integrated fluxes of F, Cl and S on the same order of magnitude, namely 3, 15 and 99 kilotonne (Gislason et al., 2002). According to Sigmarsson and Haddadi (2013), a significant fraction of the 2011 Grímsvötn magma was derived from a depth of 20 km. It was rich in sulfur gas, i.e. 630-1860 ppm, and by comparing the inclusion occurrences in clinopyroxene, plagioclase phenocrysts and in groundmass glass, the authors suggested a degassing of S of as much as 1.5 megatonne during the 2011 eruption. Our experiments indicate that about 8% of the degassed S condensed on the surfaces of the volcanic ash. The rest was emitted to the atmosphere or scrubbed into steam and melt waters. Degassing of chlorine was limited and the Cl/K ratio was constant in most glasses (Sigmarsson and Haddadi, 2013).

Similarly, the total deposition of surface F, Cl and S was estimated for the Eyjafjallajökull eruption; the data on the amount of produced ash (Gudmundsson et al., 2012b) were combined with the mean values of the released surface elements (Bagnato et al., 2013). A total of 58, 45 and 18 kilotonne of surface F, Cl and S were deposited on the ash that was released during the entire eruption. These estimates accounted for variations in the amount of deposition on the ash surface during 4 different eruption phases. The ash produced in the 2011 Grímsvötn eruption carried an order of magnitude less F and Cl but similar amounts of S.

5.4.2. Nutrients released by volcanic ash

Volcanic ash can fertilize vegetation and surface waters (e.g. Jones and Gislason (2008); Olgun et al. (2013)). The nutrients important for primary production in terrestrial environments and in the ocean are P, N, V, Mo and especially Fe (White, 1999; Frogner et al., 2001; Gislason and Eiriksdottir, 2004; Duggen et al., 2007; Jones and Gislason, 2008; Ayris and Delmelle, 2012a). The flux of nutrients from Grímsvötn was: phosphorus, 16 nmol/g; nitrate, 5.1 nmol/g; vanadium, 3.0 nmol/g; molybdenum, 0.035 nmol/g and iron, 0.96 nmol/g during the first 8 hours of water contact. The total flux of these nutrients increased only slightly over the next 15 days (Electronic Annex EA-6).

Nutrient flux was low compared to that from the previous study. Jones and Gislason (2008) reported P, 0.01-2.18 µmol/g; NO_3^- release of 0.0-13.3 µmol/g; V, 0.000-0.004 µmol/g; Mo, 0.000 µmol/g and Fe, 0.01-10.85 µmol/g, after 8 hours. This difference was explained by the pH evolution of the leachate waters. For example, P release depends strongly on pH and is scavenged in Fe phases (Jones and Gislason, 2008). We observed iron precipitates on the Grímsvötn ash while other elements were leached. The surprisingly low release of protons and some nutrients, especially iron, could be explained by Grímsvötn ash being the only phreatomagmatic ash in the comparisons, thus the sample that has considerably less surface condensates (Gislason et al., 2011b). This was confirmed by a similar flow through reactor study conducted on the phreatomagmatic ash from Eyjafjallajökull 2010 (Alfredsson et al., 2011). Alfredsson and coworkers observed elevated leachate pH and limited release of Al and Fe and concluded that phreatomagmatic ash has a highly decreased potential for fertilizing surface waters with soluble iron.

5.4.3. *Potentially harmful elements released by volcanic ash*

Some of the 51 elements released by the Grímsvötn ash have toxicity potential for aquatic environments, including F, As, Cr and Hg. Table 3 summarizes these elements and estimates the total amount released after 8 hours. These estimates do not consider the amount that could be captured within the secondary phases. Table 3 also presents the amount needed to exceed the World Health Organization (WHO, 1997; WHO, 2008) guidelines for safe drinking water and the Icelandic Directive (IcD, 1999) guidelines for surface water.

The most dangerous compounds for drinking water supplies, in order of abundance in the leachate were F, Se, Mn, As, Ni, Cd, Pb, Zn, Cr, Cu and Hg but only F and Se were likely to exceed concentrations expected to affect e.g. grassing animals (Table 3). Intake of fluoride in amounts of more than 2 to 5 mmol per kg of body weight causes risk of fluorosis and eventual death for mammals (Gessner et al., 1994; Cronin et al., 2003; WHO, 2008). The total release of F was approximately 0.72 mmol per kg of Grímsvötn

ash, so there was minimal risk of fluorosis in livestock. However, fluoride concentration as low as 0.026-0.052 mM, depending on the hardness of the water, can damage the aquatic ecosystem for invertebrates and fish (Camargo, 2003). Selenium is an essential micronutrient for humans and animals but excess intake is toxic (Presser and Ohlendorf, 1987; Hamilton, 2004; WHO, 2008; Floor and Roman-Ross, 2012). Deformity and death in embryos and hatchlings of wild aquatic birds was attributed to Se concentration of 0.0044 mM in a pond system in Kesterson National Wildlife Refuge, USA (Presser, 1994). For the Grímsvötn ash, the total Se release was approximately 0.001 mmol per kg, which is considerably lower than the Kesterson levels and therefore unlikely to be harmful for the local aquatic birds.

The most harmful elements for aqueous environments were Cu, Zn, Cd, Ni, As, Pd and Cr (Table 3). Only Cu and Zn could potentially surpass the Icelandic Directive values if surface waters were heavily contaminated by ash fall. Additional amounts of Cr, Mn, Ni, Se and Zn were released at low rates from the Grímsvötn ash after 8 hours (Electronic Annex EA-6). Still, we estimate that possibly toxic waters resulting from ash fall would be diluted by rainfall and runoff, thus decreasing risk of damage to aqueous environments.

5.5. Fragmentation processes and particle sizes

Grímsvötn erupted less than a year after the 2010 Eyjafjallajökull eruption. As a result of the Eyjafjallajökull ash plume, aviation authorities closed the air space over most of Europe because of the very fine ash that was generated during the explosive phase that started 14th of April 2010. This caused chaos, millions of travelers could not reach their destination and the airline industry worldwide suffered serious financial losses (Schumann et al., 2011). During the first days of the 2010 Eyjafjallajökull eruption, the phreatomagmatic interactions and the high magma viscosity caused intensive fragmentation resulting in production of very fine grained, sharp ash particles in the summit crater under the glacier (Gislason et al., 2011a; Gislason et al., 2011b). The basaltic magma of the Grímsvötn 2011 eruption was less viscous, which produced larger particles and the main generation of fine ash was most likely controlled by the phreatomagmatic processes. The coarser nature of the Grímsvötn ash was confirmed by a direct comparison. About 50-65% of the Grímsvötn ash sampled 50-115 km from the volcano was fine ash compared to about 68 mass % for the Eyjafjallajökull ash, sampled 50-60 km from the source (Fig. 3c and the Electronic Annex EA-4). Very fine particles (<10 µm), made up <10 mass % for the Grímsvötn ash, almost a factor of three less than for the Eyjafjallajökull ash. The measured BET surface area for the Grímsvötn ash ranged from 0.44-0.63 m^2/g, with indications of increase in surface area with distance from the eruption site (Electronic Annex EA-2). Smaller ash particles, further from the vent, is

expected and commonly observed (e.g., Fruchter et al, 1980). The ash from the explosive phase of the Eyjafjallajökull eruption had BET surface areas of 4.3 m^2/g, an order of magnitude greater, and for the effusive phase, BET surface area ranged from 0.25-0.45 m^2/g, similar to the Grímsvötn ash (Gislason et al., 2011b; Bagnato et al., 2013).

The larger particles from Grímsvötn settled faster but the eruption also produced much more ash and the plume extended more than twice the height of the Eyjafjallajökull eruption (Tesche et al., 2012). Yet, Grímsvötn caused less air traffic disturbance than the Eyjafjallajökull ash. Part of the reason is that air traffic authorities had much more information, more experience and better models so that they understood the risks and could allow higher concentration of ash in the fly zones (EC, 2010; EC, 2011). Another part of the reason is because of differences in weather and wind conditions (Gislason et al., 2011b; Gudmundsson et al., 2012b; Kristiansen et al., 2012; Tesche et al., 2012). Finally, a key factor for air travel safety was the high production of fine ash particles from highly viscous magmas and phreatomagmatic processes.

6. SUMMARY AND CONCLUSIONS

Ash produced in phreatomagmatic eruptions, such as Eyjafjallajökull 2010 and Grímsvötn 2011, have distinct characteristics that have implications for ocean fertilization, toxicity potential for humans and animals and for air travel safety. A unique series of dry, pristine ash samples, collected during the 2011 Grímsvötn eruption, shows a high fraction of fine grained, sharp particles, consisting mainly of tholeiitic glass. Six to 10 mass % of the ash that was collected 50-115 km from the volcano was very fine particles (<10 μm), harmful if inhaled.

When the ash dissolved in water, 51 elements were detected and high release rates were determined over the first 10 minutes. The initial dissolution was interpreted to be dominated by rapidly dissolving surface salts, such as $CaSO_4$, Na_2SO_4, NaCl, CaF_2, $CaCl_2$, $MgSO_4$ and $MgCl_2$. Over time, dissolution of silicate phases became more and more pronounced, causing a rise in pH to a maximum of 9.7. The flux of readily released elements from the Grímsvötn ash was low compared to those observed for other volcanic ash. The lower leachate release was attributed to the phreatomagmatic nature of the eruption, which limited the amount of surface salt condensation, especially proton salts. A relatively high pH of the reacting water further promoted precipitation of secondary aluminium, manganese and iron phases. These were suspected of scavenging Al, As, Ba, Cr, Co, Cu, Fe, Ga, Mn, Mo, Ni, P, Te, V and Zn. The limited amount of surface salts and the immobilization of some released elements in secondary phases put limits on the fertilization and toxicity potential of surface waters contaminated with volcanic ash from Grímsvötn.

The evidence produced during this study indicates that the intake of waters that had come in contact with ash would not to be dangerous for humans or animals but fluoride from the ash could have had a negative impact on aquatic life. In spite of a much larger volume of ash ejected, there was much less disruption in air traffic as a result of the 2011 Grímsvötn eruption, than during the 2010 Eyjafjallajökull eruption because the ash was coarser, weather and wind conditions were different and air traffic authorities were able to use newly developed risk standards to delineate safe fly zones.

ACKNOWLEDGEMENTS

We thank Rósa Ólafsdóttir, Eydís Salome Eiríksdóttir, Helgi Alfreðsson, Knud Dideriksen and Iwona Gałeczka for their help and encouragement. We thank the Associate Editor, Prof. Gaillardet, Dr. Delmelle and three anonymous reviewers for their constructive comments on the manuscript. The work was funded by the Nordic Volcanological Institute (NORDVULK), the Institute of Earth Sciences, Reykjavík, Iceland and the NanoGeoScience Group, Department of Chemistry, Copenhagen, Denmark.

REFERENCES

Africano F. and Bernard A. (2000) Acid alteration in the fumarolic environment of Usu volcano, Hokkaido, Japan. *J. Volcanol. Geotherm. Res.* **97**, 475-495.

Alfredsson H. A., Gislason S. R., Stipp S. L. S. and Burton K. W. (2011) Release rate of pollutants, nutrients and protons from pristine Eyjafjallajökull ash. *Mineral. Mag.* **75**, 423.

Alfredsson H. A., Opfergelt S., Burton K. W., Mokadem F., Eiriksdottir E. S. and Gislason S. R. (2012) Volcanic impact on the silicon isotope composition of natural waters during the 2010 Eyjafjallajökull eruption, S-Iceland. *Mineral. Mag.* **76**, 1414.

Allard P., Aiuppa A., Loyer H., Carrot F., Gaudry A., Pinte G., Michel A. and Dongarra G. (2000) Acid gas and metal emission rates during long-lived basalt degassing at Stromboli volcano. *Geophys. Res. Lett.* **27**, 1207-1210.

Ayris P. and Delmelle P. (2012a) Volcanic and atmospheric controls on ash iron solubility: a review. *Phys. Chem. Earth.* **45-46**, 103-112.

Ayris P. M. and Delmelle P. (2012b) The immediate environmental effects of tephra emission. *Bull. Volcanol.* **74**, 1905-1936.

Bagnato E., Aiuppa A., Bertagnini A., Bonadonna C., Cioni R., Pistolesi M., Pedone M. and Hoskuldsson A. (2013) Scavenging of sulphur, halogens and trace metals by volcanic ash: the 2010 Eyjafjallajökull eruption. *Geochim. Cosmochim. Acta* **103**, 138-160.

Bayon M. M., Alonso J. I. G. and Medel A. S. (1998) Enhanced semiquantitative multi-analysis of trace elements in environmental samples using inductively coupled plasma mass spectrometry. *J. Anal. At. Spectrom.* **13**, 277-282.

Béarat H., McKelvy M. J., Chizmeshya A. V. G., Gormley D., Nunez R., Carpenter R. W., Squires K. and Wolf G. H. (2006) Carbon sequestration via aqueous olivine mineral carbonation: role of passivating layer formation. *Environ. Sci. Technol.* **40**, 4802-4808.

Berger G., Schott J. and Loubet M. (1987) Fundamental processes controlling the first stage of alteration of a basalt glass by seawater: an experimental study between 200° and 320°C. *Earth Planet. Sci. Lett.* **84**, 431-445.

Berner R. A. (1995) Chemical weathering and its effect on atmospheric CO_2 and climate. In *Chemical Weathering Rates of Silicate Minerals, Reviews in Mineralogy* (eds. A. F. White and S. L. Brantley). Mineralogical Society of American, Washington, D. C. pp. 565-583.

Bojanowski A. (2011) Iceland's impact. *Nat. Geosci.* **4**, 732.

Brunauer S., Emmett P. H. and Teller E. (1938) Adsorption of gases in multimolecular layers. *J. Am. Chem. Soc.* **60**, 309-319.

Bursik M. I., Sparks R. S. J., Gilbert J. S. and Carey S. N. (1992) Sedimentation of tephra by volcanic plumes: I. theory and its comparison with a study of the Fogo A plinian deposit, Sao Miguel (Azores). *Bull. Volcanol.* **54**, 329-344.

Camargo J. A. (2003) Fluoride toxicity to aquatic organisms: a review. *Chemosphere* **50**, 251-264.

Cashman K. V., Sturtevant B., Papale P. and Navon O. (2000) Magmatic Fragmentation. In *Encyclopedia of Volcanoes* (ed. H. Sigurdsson). Academic Press, San Diego. pp. 421-430.

Chenet A. L., Fluteau F. and Courtillot V. (2005) Modelling massive sulphate aerosol pollution, following the large 1783 Laki basaltic eruption. *Earth Planet. Sci. Lett.* **236**, 721-731.

Cornell R. M. and Schwertmann U. (2003) *The iron oxides: structure, properties, reactions, occurrences and uses*. Wiley, Weinheim.

Cronin S. J., Neall V. E., Lecointre J. A., Hedley M. J. and Loganathan P. (2003) Environmental hazards of fluoride in volcanic ash: a case study from Ruapehu volcano, New Zealand. *J. Volcanol. Geotherm. Res.* **121**, 271-291.

Cronin S. J. and Sharp D. S. (2002) Environmental impacts on health from continuous volcanic activity at Yasur (Tanna) and Ambrym, Vanuatu. *Int. J. Environ. Health. Res.* **12**, 109-123.

de Hoog J. C. M., Koetsier G. W., Bronto S., Sriwana T. and van Bergen M. J. (2001) Sulfur and chlorine degassing from primitive arc magmas: temporal changes during the 1982-1983 eruptions of Galunggung (West Java, Indonesia). *J. Volcanol. Geotherm. Res.* **108**, 55-83.

de Moor J. M., Fischer T. P., Hilton D. R., Hauri E., Jaffe L. A. and Camacho J. T. (2005) Degassing at Anatahan volcano during the May 2003 eruption: implications from petrology, ash leachates, and SO2 emissions. *J. Volcanol. Geotherm. Res.* **146**, 117-138.

Delmelle P., Lambert M., Dufrene Y., Gerin P. and Oskarsson N. (2007) Gas/aerosol-ash interaction in volcanic plumes: new insights from surface analyses of fine ash particles. *Earth Planet. Sci. Lett.* **259**, 159-170.

Delmelle P., Villieras F. and Pelletier M. (2005) Surface area, porosity and water adsorption properties of fine volcanic ash particles. *Bull. Volcanol.* **67**, 160-169.

Duggen S., Croot P., Schacht U. and Hoffmann L. (2007) Subduction zone volcanic ash can fertilize the surface ocean and stimulate phytoplankton growth: Evidence from biogeochemical experiments and satellite data. *Geophys. Res. Lett.* **34**, L01612.

Durant A. J., Bonadonna C. and Horwell C. J. (2010) Atmospheric and environmental impact of volcanic particulates. *Elements* **6**, 235-240.

Durant A. J., Villarosa G., Rose W. I., Delmelle P., Prata A. J. and Viramonte J. G. (2012) Long-range volcanic ash transport and fallout during the 2008 eruption of Chaiten volcano, Chile. *Phys. Chem. Earth.* **45-46**, 50-64.

EC (2010) *Volcano crisis report, online report, 30 June*. European Commission, Brussels. http://ec.europa.eu/transport/ash_cloud_crisis_en.htm, 4.7.2012.

EC (2011) *Volcano Grímsvötn: How is the European response different to the Eyjafjallajökull eruption last year? FAQ, MEMO/11/346, 26 May*. European Commission, Brussels. http://ec.europa.eu/transport/ash_cloud_crisis_en.htm, 4.7.2012.

Eiriksdottir E. S., Gislason S. R. and Oelkers E. H. (2013) Does temperature or runoff control the feedback between chemical denudation and climate? Insights from NE Iceland. *Geochim. Cosmochim. Acta* **107**, 65-81.

Floor G. H. and Roman-Ross G. (2012) Selenium in volcanic environments: a review. *Appl. Geochem.* **27**, 517-531.

Flaathen T. K. and Gislason S. R. (2007) The effect of volcanic eruptions on the chemistry of surface waters: the 1991 and 2000 eruptions of Mt. Hekla, Iceland. *J. Volcanol. Geotherm. Res.* **164**, 293-316.

Flaathen T. K., Gislason S. R. and Oelkers E. H. (2010) The effect of aqueous sulphate on basaltic glass dissolution rates. *Chem. Geol.* **277**, 345-354.

Frogner P., Gislason S. R. and Oskarsson N. (2001) Fertilizing potential of volcanic ash in ocean surface water. *Geology* **29**, 487-490.

Fruchter J. S., Robertson D. E., Evans J. C., Olsen K. B., Lepel E. A., Laul J. C., Abel K. H., Sanders R. W., Jackson P. O., Wogman N. S., Perkins R. W., Vantuyl H. H., Beauchamp R. H., Shade J. W., Daniel J. L., Erikson R. L., Sehmel G. A., Lee R. N., Robinson A. V., Moss O. R., Briant J. K. and Cannon W. C. (1980) Mount St. Helens ash from the 18 May 1980 eruption: chemical, physical, mineralogical, and biological properties. *Science* **209**, 1116-1125.

Gerlach T. M. and Graeber E. J. (1985) Volatile budget of Kilauea volcano. *Nature* **313**, 273-277.

Gessner B. D., Beller M., Middaugh J. P. and Whitford G. M. (1994) Acute fluoride poisoning from a public water-system. *N. Engl. J. Med.* **330**, 95-99.

Gislason S. R., Alfredsson H. A., Eiriksdottir E. S., Hassenkam T. and Stipp S. L. S. (2011a) Volcanic ash from the 2010 Eyjafjallajökull eruption. *Appl. Geochem.* **26**, S188-S190.

Gislason S. R. and Eiriksdottir E. S. (2004) Molybdenum control of primary production in the terrestrial environment. In *Water-Rock Interaction* (eds. R. B. Wanty and R. R. Seal II). Taylor & Francis Group, London. pp. 1119-1122.

Gislason S. R. and Eugster H. P. (1987) Meteoric water-basalt interactions. 1. a laboratory study. *Geochim. Cosmochim. Acta* **51**, 2827-2840.

Gislason S. R., Hassenkam T., Nedel S., Bovet N., Eiriksdottir E. S., Alfredsson H. A., Hem C. P., Balogh Z. I., Dideriksen K., Oskarsson N., Sigfusson B., Larsen G. and Stipp S. L. S. (2011b) Characterization of Eyjafjallajökull volcanic ash particles and a protocol for rapid risk assessment. *Proc. Natl. Acad. Sci. U. S. A.* **108**, 7307-7312.

Gislason S. R. and Oelkers E. H. (2003) Mechanism, rates, and consequences of basaltic glass dissolution: II. an experimental study of the dissolution rates of basaltic glass as a function of pH and temperature. *Geochim. Cosmochim. Acta* **67**, 3817-3832.

Gislason S. R., Snorrason A., Kristmannsdottir H. K., Sveinbjornsdottir A. E., Torsander P., Olafsson J., Castet S. and Dupre B. (2002) Effects of volcanic eruptions on the CO_2 content of the atmosphere and the oceans: the 1996 eruption and flood within the Vatnajökull Glacier, Iceland. *Chem. Geol.* **190**, 181-205.

Grattan J. and Brayshay M. (1995) An amazing and portentous summer: environmental and social responses in Britain to the 1783 eruption of an Iceland volcano. *Geog. J.* **161**, 125-134.

Grattan J. P. and Gilbertson D. D. (1994) Acid-loading from Icelandic tephra falling on acidified ecosystems as a key to understanding archaeological and environmental stress in Northern and Western Britain. *J. Archaeol. Sci.* **21**, 851-859.

Gudmundsson M. T., Höskuldsson Á., Larsen G., Thordarson T., Oladottir B. A., Oddsson B., Gudnason J., Högnadottir T., Stevenson J. A., Houghton B. F., McGarvie D. and Sigurdardottir G. M. (2012a) The May 2011 eruption of Grímsvötn. *Geophys. Res. Abstr.* **14**, 12119.

Gudmundsson M. T., Thordarson T., Hoskuldsson A., Larsen G., Bjornsson H., Prata F. J., Oddsson B., Magnusson E., Hognadottir T., Petersen G. N., Hayward C. L., Stevenson J. A. and Jonsdottir I. (2012b) Ash generation and distribution from the April-May 2010 eruption of Eyjafjallajokull, Iceland. *Sci. Rep.* **2**.

Hamilton S. J. (2004) Review of selenium toxicity in the aquatic food chain. *Sci. Total Environ.* **326**, 1-31.

Horwell C. J. and Baxter P. J. (2006) The respiratory health hazards of volcanic ash: a review for volcanic risk mitigation. *Bull. Volcanol.* **69**, 1-24.

IcD (1999) *Reglugerð: um varnir gegn mengun vatns*. Icelandic Directive, Reykjavík. http://www.reglugerd.is/interpro/dkm/Webguard.nsf/lookByNumer/7961999?OpenDocument, 4.7.2012.

International Center for Diffraction Data (1995) *PDF-2 Sets 1-45 database*, Newtown Square, PA 19073, USA.

Jaycock M. J. and Parfitt G. D. (1981) *Chemistry of interfaces*. Ellis Horwood, Chichester.

Jones M. T. and Gislason S. R. (2008) Rapid releases of metal salts and nutrients following the deposition of volcanic ash into aqueous environments. *Geochim. Cosmochim. Acta* **72**, 3661-3680.

Kinniburgh D. G., Jackson M. L. and Syers J. K. (1976) Adsorption of alkaline earth, transition, and heavy metal cations by hydrous oxide gels of iron and aluminum. *Soil Sci. Soc. Am. J.* **40**, 796-799.

Kinniburgh D. G., Syers J. K. and Jackson M. L. (1975) Specific adsorption of trace amounts of calcium and strontium by hydrous oxides of iron and aluminum. *Soil Sci. Soc. Am. J.* **39**, 464-470.

Kristiansen N. I., Stohl A., Prata A. J., Bukowiecki N., Dacre H., Eckhardt S., Henne S., Hort M. C., Johnson B. T., Marenco F., Neininger B., Reitebuch O., Seibert P., Thomson D. J., Webster H. N. and Weinzierl B. (2012) Performance assessment of a volcanic ash transport model mini-ensemble used for inverse modeling of the 2010 Eyjafjallajökull eruption. *J. Geophys. Res.* **117**.

Lathem T. L., Kumar P., Nenes A., Dufek J., Sokolik I. N., Trail M. and Russell A. (2011) Hygroscopic properties of volcanic ash. *Geophys. Res. Lett.* **38**, L11802.

Le Blond J. S., Horwell C. J., Baxter P. J., Michnowicz S. A. K., Tomatis M., Fubini B., Delmelle P., Dunster C. and Patia H. (2010) Mineralogical analyses and in vitro screening tests for the rapid evaluation of the health hazard of volcanic ash at Rabaul volcano, Papua New Guinea. *Bull. Volcanol.* **72**, 1077-1092.

Lee G., Bigham J. M. and Faure G. (2002) Removal of trace metals by coprecipitation with Fe, Al and Mn from natural waters contaminated with acid mine drainage in the Ducktown Mining District, Tennessee. *Appl. Geochem.* **17**, 569-581.

Lieke K. I., Kristensen T. B., Korsholm U. S., Sørensen J. H., Kandler K., Weinbruch S., Ceburnis D., Ovadnevaite J., O'Dowd C. D. and Bilde M. (2013) Characterization of volcanic ash from the 2011 Grímsvötn eruption by means of single-particle analysis. *Atmos. Environ.* **79**, 411-420.

Mahowald N. M., Baker A. R., Bergametti G., Brooks N., Duce R. A., Jickells T. D., Kubilay N., Prospero J. M. and Tegen I. (2005) Atmospheric global dust cycle and iron inputs to the ocean. *Glob. Biogeochem. Cycles* **19**.

Martin R. S., Wheeler J. C., Ilyinskaya E., Braban C. F. and Oppenheimer C. (2012) The uptake of halogen (HF, HCl, HBr and HI) and nitric (HNO3) acids into acidic sulphate particles in quiescent volcanic plumes. *Chem. Geol.* **296–297**, 19-25.

Mather T. A., Witt M. L. I., Pyle D. M., Quayle B. M., Aiuppa A., Bagnato E., Martin R. S., Sims K. W. W., Edmonds M., Sutton A. J. and Ilyinskaya E. (2012) Halogens and trace metal emissions from the ongoing 2008 summit eruption of Kilauea volcano, Hawaii. *Geochim. Cosmochim. Acta* **83**, 292-323.

McKenzie R. M. (1980) Adsorption of lead and other heavy metals on oxides of manganese and iron. *Aust. J. Soil Res.* **18**, 61-73.

Moulder J. F., Stickle W. F., Sobol P. E. and Bomben K. D. (1995) *Handbook of X-ray Photoelectron Spectroscopy*. Physical Electronics, Minnesota.

Moune S., Gauthier P. J. and Delmelle P. (2010) Trace elements in the particulate phase of the plume of Masaya Volcano, Nicaragua. *J. Volcanol. Geotherm. Res.* **193**, 232-244.

Naughton J. J., Lewis V. A., Hammond D. and Nishimot D. (1974) The chemistry of sublimates collected directly from lava fountains at Kilauea Volcano, Hawaii. *Geochim. Cosmochim. Acta* **38**, 1679-1690.

Nesbitt H. W., Bancroft G. M., Davidson R., McIntyre N. S. and Pratt A. R. (2004) Minimum XPS core-level line widths of insulators, including silicate minerals. *Am. Miner.* **89**, 878-882.

Oelkers E. H. and Gislason S. R. (2001) The mechanism, rates and consequences of basaltic glass dissolution: I. An experimental study of the dissolution rates of basaltic glass as a function of aqueous Al, Si and oxalic acid concentration at 25°C and pH = 3 and 11. *Geochim. Cosmochim. Acta* **65**, 3671-3681.

Okazaki M., Takamidoh K. and Yamane I. (1986) Adsorption of heavy metal cations on hydrated oxides and oxides of iron and aluminum with different crystallinities. *Soil Sci. Plant Nutr.* **32**, 523-533.

Olgun N., Duggen S., Andronico D., Kutterolf S., Croot P. L., Giammanco S., Censi P. and Randazzo L. (2013) Possible impacts of volcanic ash emissions of Mount Etna on the primary productivity in the oligotrophic Mediterranean Sea: results from nutrient-release experiments in seawater. *Mar. Chem.* **152**, 32-42.

Olgun N., Duggen S., Croot P. L., Delmelle P., Dietze H., Schacht U., Oskarsson N., Siebe C., Auer A. and Garbe-Schonberg D. (2011) Surface ocean iron fertilization: the role of airborne volcanic ash from subduction zone and hot spot volcanoes and related iron fluxes into the Pacific Ocean. *Glob. Biogeochem. Cycle* **25**.

Olsson J., Bovet N., Makovicky E., Bechgaard K., Balogh Z. and Stipp S. L. S. (2012) Olivine reactivity with CO_2 and H_2O on a microscale: implications for carbon sequestration. *Geochim. Cosmochim. Acta* **77**, 86-97.

Oman L., Robock A., Stenchikov G. L., Thordarson T., Koch D., Shindell D. T. and Gao C. C. (2006) Modeling the distribution of the volcanic aerosol cloud from the 1783-1784 Laki eruption. *J. Geophys. Res.* **111**.

Oskarsson N. (1980) The interaction between volcanic gases and tephra: fluorine adhering to tephra of the 1970 Hekla eruption. *J. Volcanol. Geotherm. Res.* **8**, 251-266.

Parkhurst D. L. and Appelo C. A. J. (1999) User's guide to PHREEQC (version 2) — a computer program for speciation, batch-reaction, one-dimensional transport, and inverse geochemical calculations. *U.S. Geological Survey Water Resources Investigation Report* **99-4259**.

Pavlova V. and Sigg L. (1988) Adsorption of trace metals on aluminum oxide: a simulation of processes in freshwater systems by close approximation to natural conditions. *Wat. Res.* **22**, 1571-1575.

Pentecost A. (2005) *Travertine*. Springer, London.
Petersen G. N., Bjornsson H., Arason P. and von Löwis S. (2012) Two weather radar time series of the altitude of the volcanic plume during the May 2011 eruption of Grímsvötn, Iceland. *Earth Syst. Sci. Data* **4**, 121-127.
Presser T. S. (1994) The Kesterson effect. *Environ. Manage.* **18**, 437-454.
Presser T. S. and Ohlendorf H. M. (1987) Biogeochemical cycling of selenium in the San Joaquin Valley, California, USA. *Environ. Manage.* **11**, 805-821.
Robock A. (2000) Volcanic eruptions and climate. *Rev. Geophys.* **38**, 191-219.
Rose W. I. (1977) Scavenging of volcanic aerosol by ash: atmospheric and volcanologic implications. *Geology* **5**, 621-624.
Rose W. I., Chuan R. L., Cadle R. D. and Woods D. C. (1980) Small particles in volcanic eruption clouds. *Am. J. Sci.* **280**, 671-696.
Rust A. C. and Cashman K. V. (2011) Permeability controls on expansion and size distributions of pyroclasts. *J. Geophys. Res.-Solid Earth* **116**, B11202.
Schott J. and Berner R. A. (1983) X-ray photoelectron studies of the mechanism of iron silicate dissolution during weathering. *Geochim. Cosmochim. Acta* **47**, 2233-2240.
Schumann U., Weinzierl B., Reitebuch O., Schlager H., Minikin A., Forster C., Baumann R., Sailer T., Graf K., Mannstein H., Voigt C., Rahm S., Simmet R., Scheibe M., Lichtenstern M., Stock P., Ruba H., Schauble D., Tafferner A., Rautenhaus M., Gerz T., Ziereis H., Krautstrunk M., Mallaun C., Gayet J. F., Lieke K., Kandler K., Ebert M., Weinbruch S., Stohl A., Gasteiger J., Gross S., Freudenthaler V., Wiegner M., Ansmann A., Tesche M., Olafsson H. and Sturm K. (2011) Airborne observations of the Eyjafjalla volcano ash cloud over Europe during air space closure in April and May 2010. *Atmos. Chem. Phys.* **11**, 2245-2279.
Shirley D. A. (1972) High-resolution X-ray photoemission spectrum of valence bands of gold. *Phys. Rev. B* **5**, 4709-4714.
Sigmarsson O. and Haddadi B. (2013) The 2011 Grímsvötn eruption and the size of Grímsvötn eruptions (abstr). *Spring meeting of the Icelandic Geological Society*, Reykjavík. pp. 27-28.
Sparks R. S. J. (1978) The dynamics of bubble formation and growth in magmas: a review and analysis. *J. Volcanol. Geotherm. Res.* **3**, 1-37.
Sposito G. (1995) *The environmental chemistry of aluminum*. CRC Press, Berkeley.
Stefansdottir M. B. and Gislason S. R. (2005) The erosion and suspended matter/seawater interaction during and after the 1996 outburst flood from the Vatnajokull Glacier, Iceland. *Earth Planet. Sci. Lett.* **237**, 433-452.
Stipp S. L. and Hochella M. F. (1991) Structure and bonding environments at the calcite surface as observed with X-ray photoelectron spectroscopy (XPS) and low energy electron diffraction (LEED). *Geochim. Cosmochim. Acta* **55**, 1723-1736.
Stipp S. L. S., Gutmannsbauer W. and Lehmann T. (1996) The dynamic nature of calcite surfaces in air. *Am. Miner.* **81**, 1-8.
Stockmann G. J., Wolff-Boenisch D., Gislason S. R. and Oelkers E. H. (2011) Do carbonate precipitates affect dissolution kinetics? 1: basaltic glass. *Chem. Geol.* **284**, 306-316.
Stumm W. and Morgan J. J. (1996) *Aquatic chemistry: chemical equilibria and rates in natural waters*. Wiley, New York.
Takahashi T., Sutherland S. C., Wanninkhof R., Sweeney C., Feely R. A., Chipman D. W., Hales B., Friederich G., Chavez F., Sabine C., Watson A., Bakker D. C. E., Schuster U., Metzl N., Yoshikawa-Inoue H., Ishii M., Midorikawa T., Nojiri Y., Kortzinger A., Steinhoff T., Hoppema M., Olafsson J., Arnarson T. S., Tilbrook B., Johannessen T., Olsen A., Bellerby

R., Wong C. S., Delille B., Bates N. R. and de Baar H. J. W. (2009) Climatological mean and decadal change in surface ocean pCO_2, and net sea-air CO_2 flux over the global oceans. *Deep Sea Res. Part II* **56**, 554-577.

Taylor H. E. and Lichte F. E. (1980) Chemical composition of Mount St. Helens volcanic ash. *Geophys. Res. Lett.* **7**, 949-952.

Taylor P. S. and Stoiber R. E. (1973) Soluble material on ash from active Central American volcanoes. *Geol. Soc. Am. Bull.* **84**, 1031-1041.

Tesche M., Glantz P., Johansson C., Norman M., Hiebsch A., Ansmann A., Althausen D., Engelmann R. and Seifert P. (2012) Volcanic ash over Scandinavia originating from the Grímsvötn eruptions in May 2011. *J. Geophys. Res.* **117**.

Tester J. W., Worley W. G., Robinson B. A., Grigsby C. O. and Feerer J. L. (1994) Correlating quartz dissolution kinetics in pure water from 25 to 625°C. *Geochim. Cosmochim. Acta* **58**, 2407-2420.

Thorbergsdottir I. M. and Gislason S. R. (2004) Internal loading of nutrients and certain metals in the shallow eutrophic Lake Myvatn, Iceland. *Aquat. Ecol.* **38**, 191-207.

Thordarson T. and Hoskuldsson A. (2008) Postglacial volcanism in Iceland. *Jökull* **58**, 197-228.

Thordarson T. and Larsen G. (2007) Volcanism in Iceland in historical time: volcano types, eruption styles and eruptive history. *J. Geodyn.* **43**, 118-152.

Thordarson T. and Self S. (1996) Sulfur, chlorine and fluorine degassing and atmospheric loading by the Roza eruption, Columbia River Basalt Group, Washington, USA. *J. Volcanol. Geotherm. Res.* **74**, 49-73.

Thordarson T. and Self S. (2003) Atmospheric and environmental effects of the 1783-1784 Laki eruption: a review and reassessment. *J. Geophys. Res.* **108**.

Tómasson H. (1996) The jökulhlaup from Katla in 1918. *Ann. Glaciol.* **22**, 249-254.

White D. (1999) *The physiology and biochemistry of prokaryotes*. Oxford University Press, Oxford.

WHO (1997) *Aluminium, environmental health criteria 194*. International Programme on Chemical Safety, World Health Organization, Geneva.

WHO (2008) *Guidelines for drinking-water quality*. World Health Organization, Geneva.

Witham C. S., Oppenheimer C. and Horwell C. J. (2005) Volcanic ash-leachates: a review and recommendations for sampling methods. *J. Volcanol. Geotherm. Res.* **141**, 299-326.

Wogelius R. A. and Walther J. V. (1992) Olivine dissolution kinetics at near-surface conditions. *Chem. Geol.* **97**, 101-112.

Wolff-Boenisch D., Gislason S. R. and Oelkers E. H. (2004a) The effect of fluoride on the dissolution rates of natural glasses at pH 4 and 25°C. *Geochim. Cosmochim. Acta* **68**, 4571-4582.

Wolff-Boenisch D., Gislason S. R., Oelkers E. H. and Putnis C. V. (2004b) The dissolution rates of natural glasses as a function of their composition at pH 4 and 10.6, and temperatures from 25 to 74°C. *Geochim. Cosmochim. Acta* **68**, 4843-4858.

Zakaznova-Herzog V. P., Nesbitt H. W., Bancroft G. M. and Tse J. S. (2006) High resolution core and valence band XPS spectra of non-conductor pyroxenes. *Surf. Sci.* **600**, 3175-3186.

Zakaznova-Herzog V. P., Nesbitt H. W., Bancroft G. M. and Tse J. S. (2008) Characterization of leached layers on olivine and pyroxenes using high-resolution XPS and density functional calculations. *Geochim. Cosmochim. Acta* **72**, 69-86.

Zakaznova-Herzog V. P., Nesbitt H. W., Bancroft G. M., Tse J. S., Gao X. and Skinner W. (2005) High-resolution valence-band XPS spectra of the nonconductors quartz and olivine. *Phys. Rev. B* **72**, 205113.

Tables

Table 1. Sample location and weather conditions for the Grímsvötn ash samples. Most of the total ash ejected had already been released when sampling began. The sampling was completed within an interval of only 3 hours and before the first rain fell on the ash.

Sample	Location (latitude and longitude)		Distance to eruption site (km)	Sampling time 22.05.11 (GMT)	Ash thickness (mm)	Nearest weather station	Temp (°C)	Humidity (%)	Wind speed (m/s)
1	63°32'43.4"	18°27'05.4"	115	16:05	< 1	Mýrd.	5.4	60	5.5
2	63°37'17.6"	18°26'50.0"	107	16:25	< 1	Mýrd.	5.5	59	5.1
3	63°42'55.6"	18°15'32.6"	93.2	16:55	2	Kirkj.	5.8	53	1.7
4	63°47'12.1"	18°02'09.2"	81.2	17:30	10	Kirkj.	6.3	49	1.8
5	63°47'43.4"	18°02'12.8"	79.4	17:55	8	Kirkj.	6.8	44	1.8
6	63°51'06.5"	17°53'26.4"	70.7	18:10	10	Kirkj.	6.8	44	1.8
7	63°53'54.3"	17°44'11.8"	62.1	18:33	15	Lómag.	5.5	68	2.5
8	63°58'30.1"	17°00'49.2"	50.4	19:30	3	Skaftaf.	5.2	73	2.0

Table 2. Composition of Grímsvötn Sample #8 expressed as oxide wt %. Surface composition was determined before and after 15 days of exposure to deionised water in a flow reactor. The energy of the peak used for quantification is shown in brackets. Carbon contamination, detected on all surfaces, was excluded for clearer comparison. XPS data are presented in atom % in the Electronic Annex EA-5, including F and Cl.

	Microprobe (single phases)		**XRF (bulk)**	**XPS (surface)**	
Oxide wt %	**Plagioclase**	**Glass**		**Pristine**	**Water exposed**
SiO_2	51.87	50.66	50.20	60.0 (102.7 eV)	62.0 (103.1 eV)
Al_2O_3	29.07	13.34	13.46	13.8 (74.5 eV)	16.1 (74.9 eV)
FeO	1.11	13.56	13.64	7.5 (711.4 eV)	10.6 (711.6 eV)
CaO	13.16	9.68	9.90	7.0 (347.9 eV)	4.7 (348.5 eV)
MgO	0.27	5.46	5.58	4.2 (50.2 eV)	2.5 (50.9 eV)
TiO_2	0.15	2.90	2.85	1.7 (458.4 eV)	3.4 (458.6 eV)
Na_2O	4.05	2.87	2.78	3.2 (1072.6 eV)	0.7 (1072.9 eV)
K_2O	0.09	0.50	0.55	BDL	BDL
MnO	0.02	0.21	0.23	BDL	BDL
S_{total}	NA	NA	0.08	2.7 (169.5 eV)	<0.5
Total	99.77	99.17	100.30	100	100

NA, not analyzed; BDL, below detection limit.

Table 3. The contamination potential for Grímsvötn Sample #8. Toxic elements that could be released into surface waters within 8 hours. The WHO standard for drinking water and the Icelandic Directive for surface waters are shown for comparison. There are no threshold values for Al.

Element	Amount released (pmol/g (ash))	WHO threshold[a] (nmol/L)	Iceland Directorate threshold[a] (nmol/L)	Amount to exceed WHO threshold (kg (ash)/L)	Amount to exceed IcD threshold (kg (ash)/L)
As	34	133	67	3.9	1.9
Cd	1.3	27	1	20	0.67
Cr	19	960	96	51	5
Cu	170	31000	47	180	0.27
F	720000	79000	NTV	0.11	-
Hg	0.060	30	NTV	500	-
Mn	7100	7300	NTV	1.0	-
Ni	153	1200	256	7.8	1.7
Pb	1.5	48	5	33	3.3
Se	1000	130	NTV	0.13	-
Zn	1100	46000	306	41	0.27

NTV, no threshold value.

[a] The threshold values were published by World Health Organization for drinking water (WHO, 2008) and the Icelandic Directive for surface waters, defining the lower limits for effects on sensitive biota, Category III (IcD, 1999).

Figure Captions

Fig. 1. The location of the Grímsvötn eruption (red star) under the Vatnajökull glacier, weather stations (black circles) and the sample collection sites (red triangles). The ash samples were collected across the major axis of the fallout, along the main road in southeastern Iceland, 50-115 km south/southwest from the summit. They represent the main fallout during the first 21 to 24 hours of the eruption, when the effusive rate was highest and the plum rose to more than 10 km.

Fig. 2. The plug flow reactor. Ultrapure deionised (MilliQ) water was pumped into a Teflon, flow through reactor (1) holding the ash (4). The effluent was collected as samples (2) or directed into a plastic tube (3) for in line pH measurements. (5) Nylon sieves, (6) 0.2 µm cellulose acetate membrane filters and (7) a 3 way valve were also used.

Fig. 3. The pristine ash Sample #8. Electron microprobe (EMPA) backscattered image (a), scanning electron microscopy (SEM) image (b) and the particle size distribution (c) show that the ash was fine grained and sharp. The grain size distribution of the phreatomagmatic explosive ash from the 2010 Eyjafjallajökull eruption is included for comparison. The darkest grey shaded area represents the mass % overlap of the two samples. The threshold for particles classified as fine ash (<63 µm) and the size that constitutes increased risk when inhaled (<10 µm) are indicated with dashed lines. The Grímsvötn ash is coarser than that from the explosive phase of Eyjafjallajökull.

Fig. 4. Release per gram of Grímsvötn ash Sample #8 as function of time. The release rate of the major elements (a), anions and protons (b), transition metals (c) and selected nutrients (d) were monitored for 15 days. Dashed lines indicate the limit of quantification. The release rate of Si (CSiR), resulting from bulk dissolution of basaltic glass calculated using the procedure of Gislason and Oelkers (2003), is shown for comparison.

Fig. 5. The total alkalinity (a) and the saturation state of selected minerals (b) modelled with PHREEQC. The net alkalinity did not change during dissolution of the salt condensates but alkalinity increased during glass dissolution. The alkalinity decrease after about 100 minutes resulted from decrease in bulk dissolution rates of the volcanic glass. The saturation states of the aluminium, iron and manganese phases were controlled by pH.

Fig. 6. Surface composition of Sample #8, measured with X-ray photoelectron spectroscopy (XPS), versus bulk composition, measured with X-ray fluorescence (XRF) before (closed symbols) and after (open symbols) 15 days of water exposure.

Figure1
Click here to download high resolution image

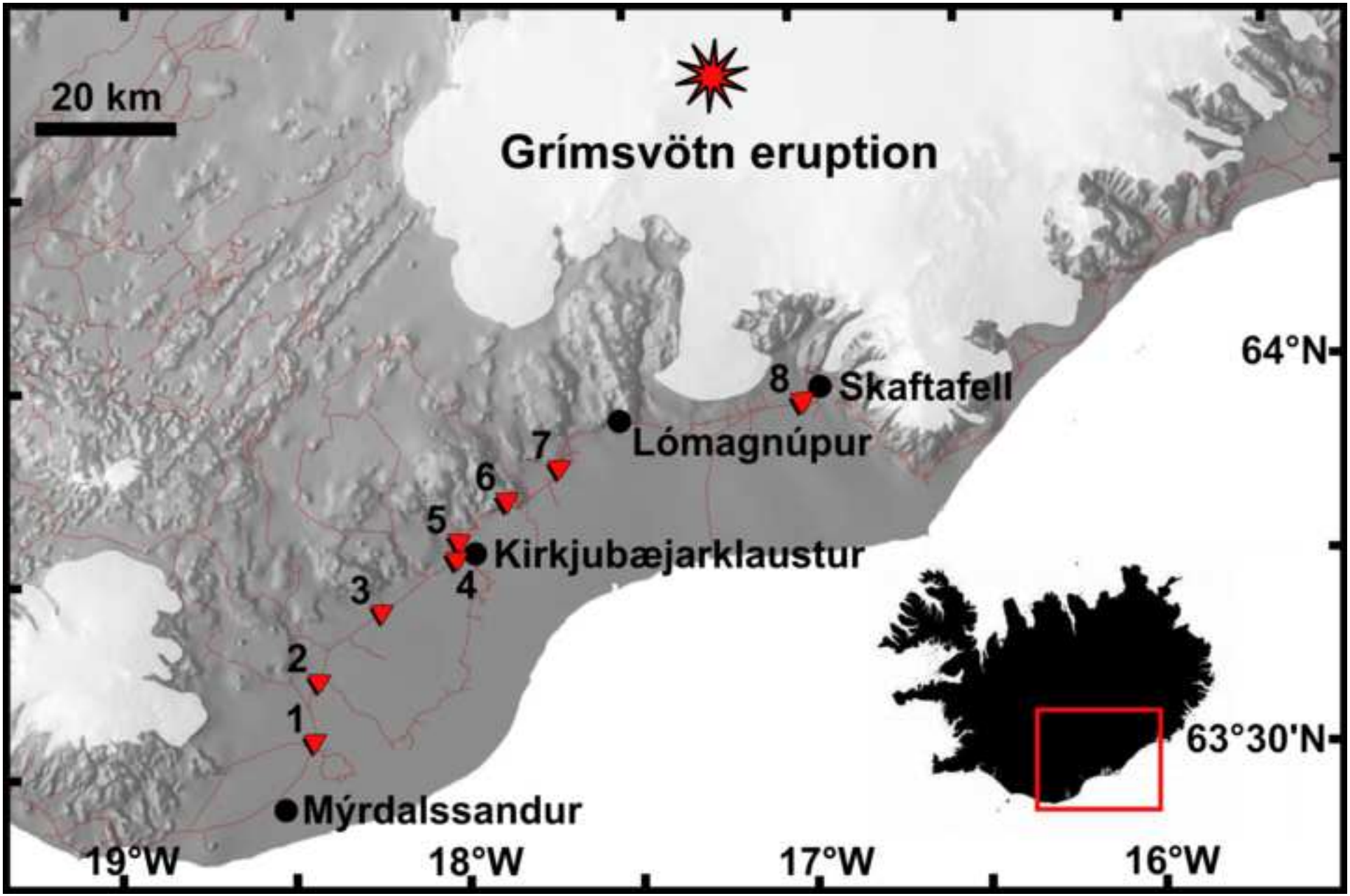

Figure2

Click here to download high resolution image

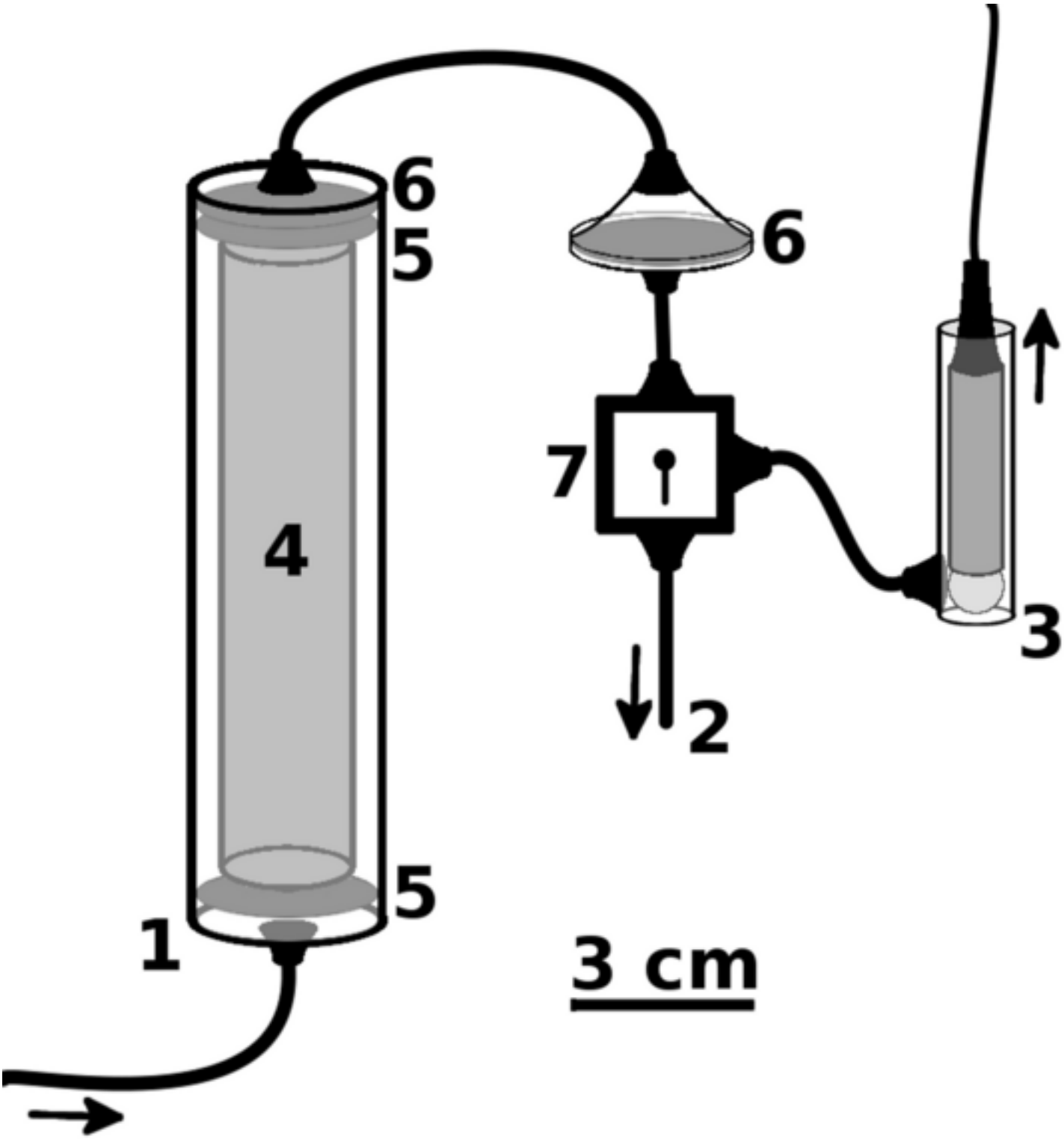

Figure3

Click here to download high resolution image

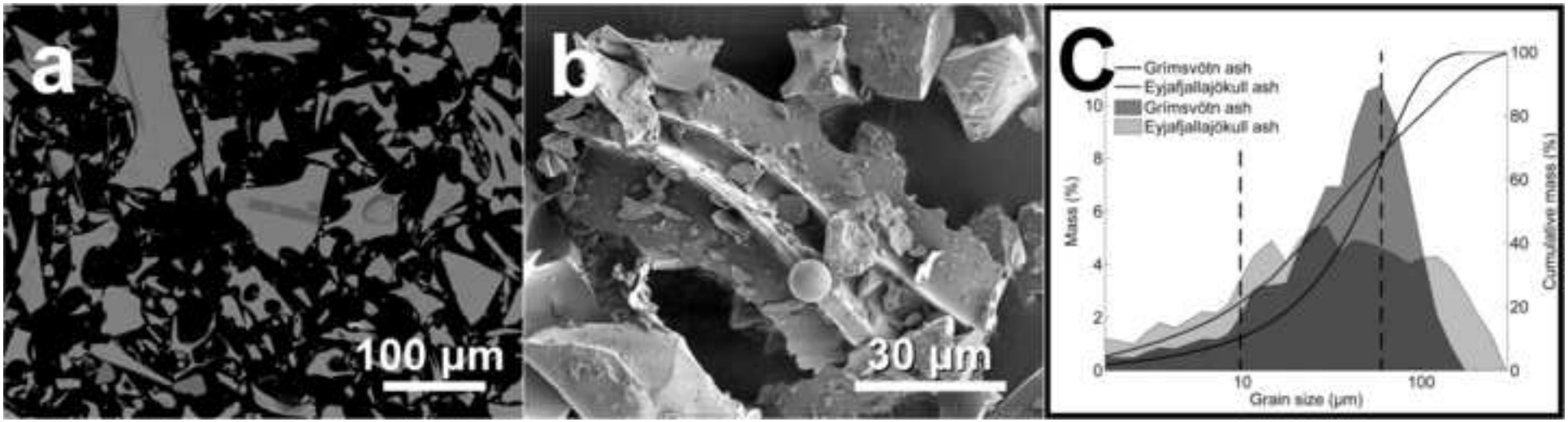

Figure4

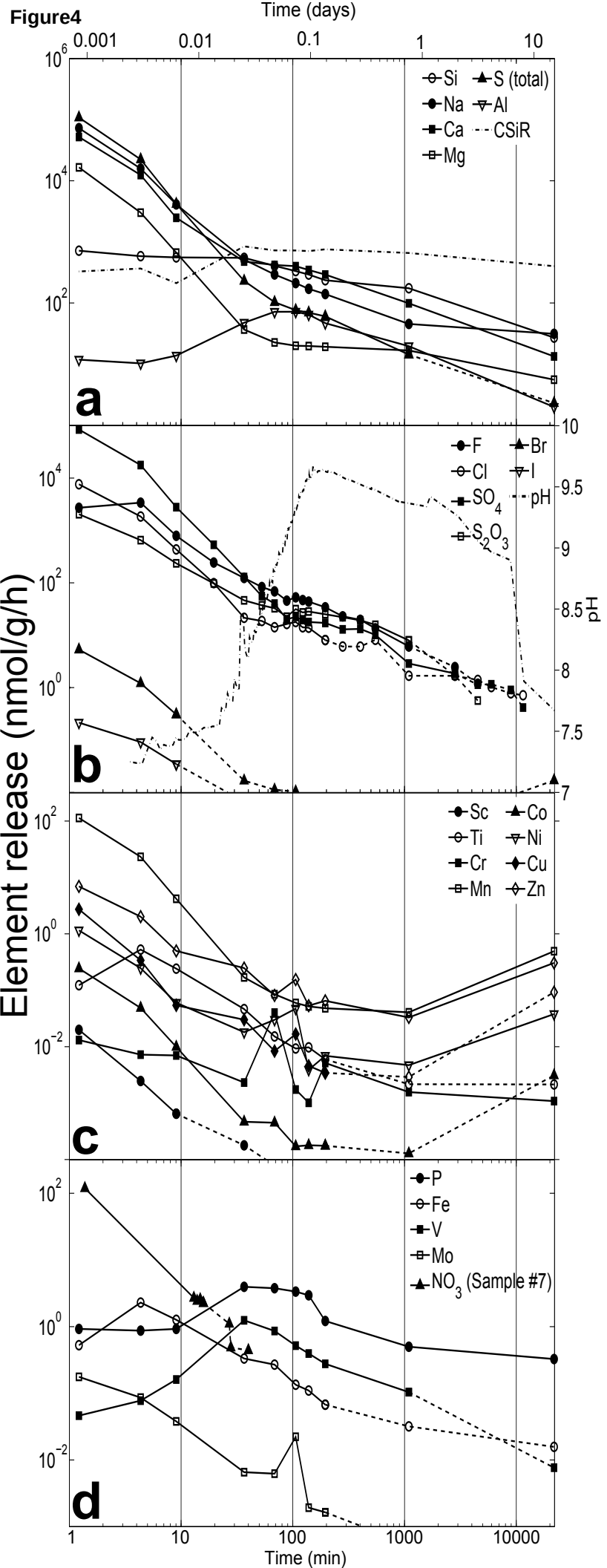
Time (days)
0.001
0.01
0.1
1
10
Si
S (total)
Na
Al
Ca
CSiR
Mg
a
F
Br
Cl
I
SO4
pH
S2O3
b
pH
Sc
Co
Ti
Ni
Cr
Cu
Mn
Zn
c
P
Fe
V
Mo
NO3 (Sample #7)
d
Element release (nmol/g/h)
1
10
100
1000
10000
Time (min)

Figure5

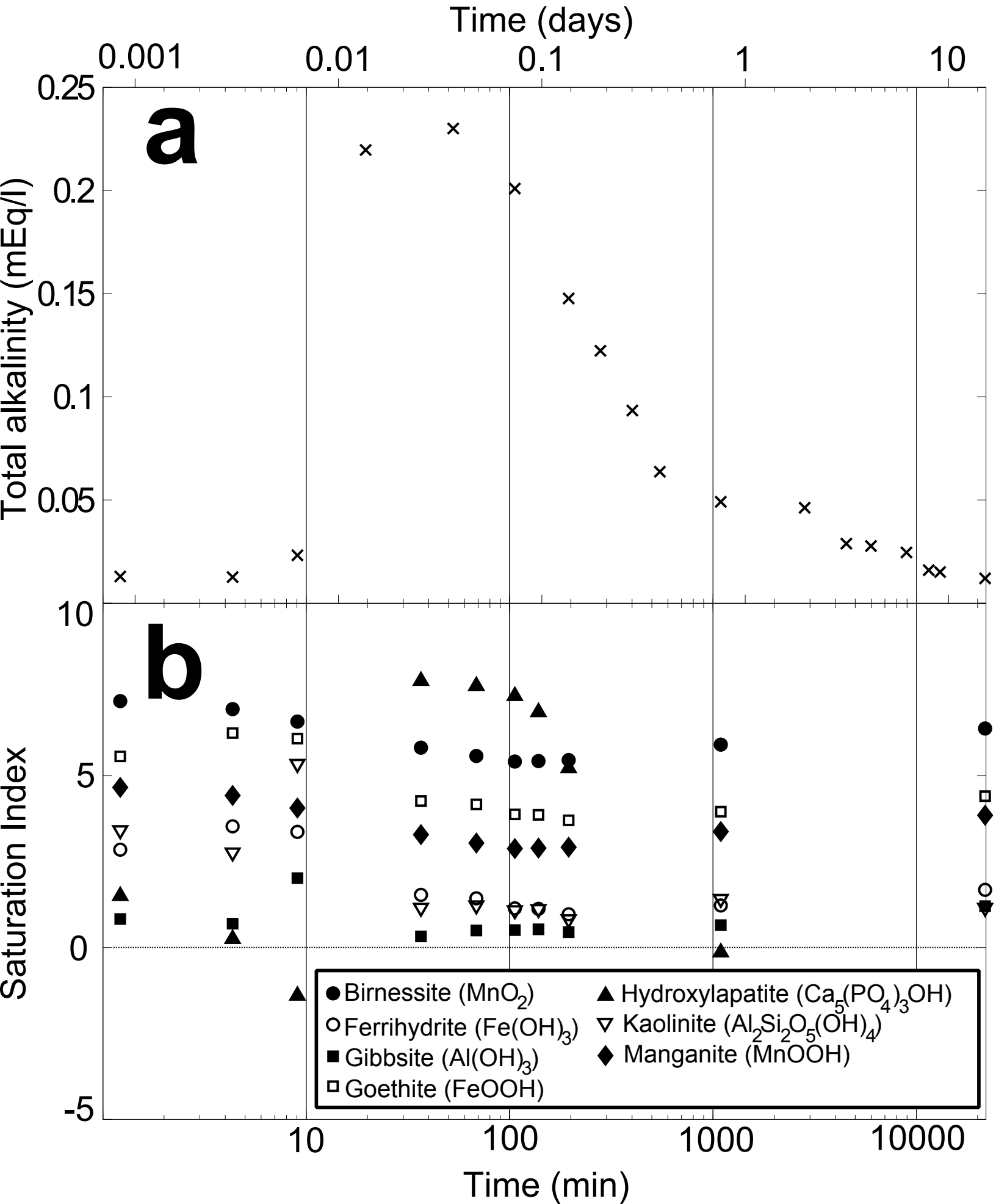
Time (days)
0.001
0.01
0.1
1
10
a
Total alkalinity (mEq/l)
0.25
0.2
0.15
0.1
0.05
0
b
Saturation Index
10
5
0
-5
Birnessite (MnO_2)
Ferrihydrite ($Fe(OH)_3$)
Gibbsite ($Al(OH)_3$)
Goethite (FeOOH)
Hydroxylapatite ($Ca_5(PO_4)_3OH$)
Kaolinite ($Al_2Si_2O_5(OH)_4$)
Manganite (MnOOH)
10
100
1000
10000
Time (min)

Figure6

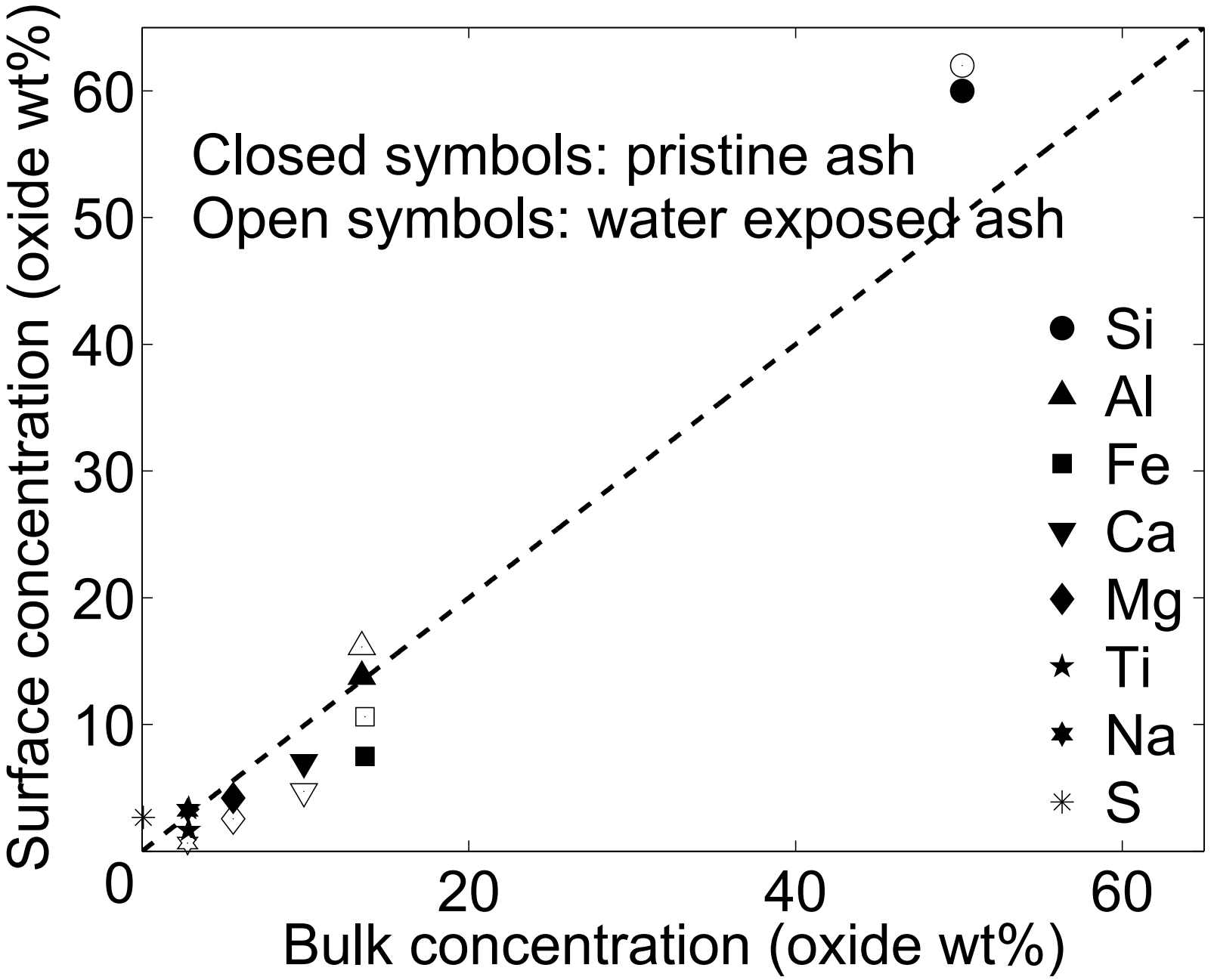
Surface concentration (oxide wt%)
Bulk concentration (oxide wt%)
0
10
20
30
40
50
60
0
20
40
60
Closed symbols: pristine ash
Open symbols: water exposed ash
Si
Al
Fe
Ca
Mg
Ti
Na
S

Electronic Annex EA-1: XRF data

wt%	MDL	Ash sample #1	Ash sample #7	Ash sample #8
LOI	-5.11	-0.91	-0.94	-0.78
SiO2	0.1	49.6	50.2	50.2
Al2O3	0.01	13.21	13.41	13.46
Fe2O3	0.01	15.04	15.23	15.16
CaO	0.01	9.71	9.81	9.9
MgO	0.01	5.5	5.53	5.58
Na2O	0.01	2.78	2.83	2.78
K2O	0.01	0.56	0.53	0.55
MnO	0.01	0.23	0.23	0.23
TiO2	0.01	2.85	2.86	2.85
P2O5	0.01	0.31	0.31	0.31
Cr2O3	0.001	0.007	0.007	0.004
Ba	0.01	0.02	<0,01	0.01
Cu	0.001	0.006	0.008	0.004
Ni	0.001	0.002	<0,001	0.001
Pb	0.001	<0,001	<0,001	<0,001
Sr	0.002	0.022	0.022	0.019
Zn	0.001	0.012	0.011	0.012
Zr	0.002	0.016	0.015	0.016
SO3	0.002	0.148	0.154	0.142
V2O5	0.002	0.075	0.077	0.072
C (total)	0.02	<0,02	<0,02	<0,02
S (total)	0.02	0.09	0.12	0.08
SUM		**98.9**	**99.99**	**100.3**

Electronic Annex EA-2: BET data

Ash sample #	BET instrument	Degasssing temperature (°C)	BET surface area (m^2/g)	Distance to eruption site (km)	Geometric specific surface area (m^2/g)	Roughness factor
1	Tristar	150	0.63	115.08	0.073	8.7
2	Tristar	150	0.6	107.05	NA	
3	Tristar	150	0.59	93.17	NA	
4	Tristar	150	0.53	81.17	NA	
5	Tristar	150	0.59	79.42	NA	
6	Tristar	150	0.44	70.68	0.077	5.7
7	Tristar	150	0.54	62.13	NA	
8	Tristar	150	0.51	50.37	0.092	5.5
1	QN	-	0.43	115.08		
1	QN	60	0.64	115.08		
1	QN	90	0.61	115.08		
1	QN	90	0.66	115.08		
1	QN	150	0.64	115.08		
1	QN	200	0.64	115.08		
1	QN	200	0.64	115.08		
8	QN	-	0.41	50.37		
8	QN	60	0.59	50.37		
8	QN	90	0.54	50.37		
8	QN	90	0.59	50.37		
8	QN	150	0.56	50.37		
8	QN	200	0.58	50.37		
8	QN	200	0.52	50.37		

NA, not available; Tristar, Tristar 3000; QN, Quantachrome Nova 2200.

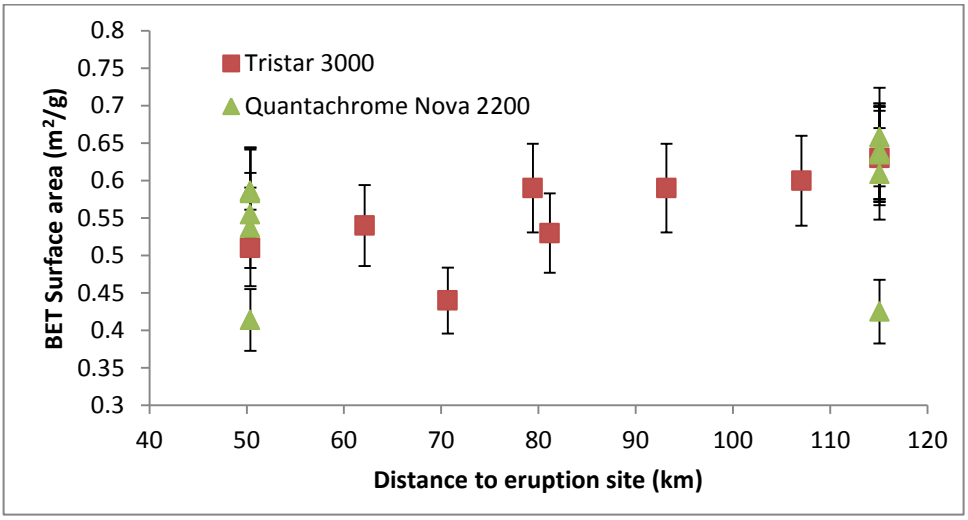

Electronic Annex EA-3: Reactor effluent chemistry

pH, Ash sample #8								
Sampl.	**pH**	**Temp. (°C)**	**Sampl.**	**pH**	**Temp. (°C)**	**Sampl.**	**pH**	**Temp. (°C)**
3.5	7.25	23.4	**58**	8.6	20.6	**125**	9.47	20.6
4	7.24	23.4	**59**	8.59	20.6	**126**	9.51	20.7
4.5	7.24	23.4	**60**	8.63	20.6	**128**	9.51	20.6
5	7.35	23.4	**61**	8.64	20.6	**129**	9.52	20.6
5.5	7.45	23.4	**62**	8.72	20.5	**130**	9.55	20.7
6	7.42	23.4	**63**	8.69	20.5	**131**	9.55	20.7
6.5	7.35	23.4	**64**	8.69	20.6	**132**	9.55	20.6
7	7.39	23.4	**65**	8.73	20.6	**133**	9.55	20.6
7.5	7.38	23.5	**66**	8.72	20.6	**134**	9.57	20.7
8	7.38	23.5	**67**	8.82	20.6	**136**	9.57	20.7
8.5	7.39	23.5	**68**	8.81	20.6	**137**	9.56	20.7
9	7.45	23.5	**70**	8.87	20.6	**138**	9.56	20.7
9.5	7.43	23.5	**71**	8.86	20.6	**140**	9.6	20.8
10	7.43	23.5	**72**	8.86	20.6	**141**	9.58	20.7
11	7.44	23.5	**73**	8.89	20.6	**144**	9.58	20.7
12	7.51	23.5	**74**	8.89	20.6	**145**	9.58	20.7
13	7.49	23.4	**76**	8.95	20.7	**146**	9.6	20.7
14	7.49	23.3	**77**	8.94	20.6	**147**	9.6	20.7
16	7.53	23.2	**78**	8.93	20.6	**150**	9.6	20.8
17	7.53	23	**79**	8.96	20.6	**151**	9.66	20.8
18	7.53	22.7	**80**	8.96	20.6	**152**	9.66	20.8
19	7.54	22.5	**82**	9.04	20.6	**153**	9.66	20.8
20	7.54	22.3	**83**	9.03	20.6	**156**	9.66	20.7
21	7.55	22.1	**84**	9.02	20.6	**157**	9.66	20.7
22	7.55	21.9	**85**	9.02	20.7	**158**	9.64	20.8
23	7.69	22	**86**	9.09	20.7	**161**	9.64	20.8
24	7.67	21.9	**87**	9.08	20.7	**163**	9.64	20.7
25	7.67	21.9	**88**	9.07	20.7	**164**	9.63	20.8
26	7.81	21.9	**89**	9.07	20.7	**166**	9.62	20.7
27	7.76	21.8	**90**	9.17	20.7	**169**	9.63	20.7
28	7.75	21.7	**92**	9.15	20.7	**172**	9.63	20.7
30	7.93	21.5	**93**	9.18	20.7	**175**	9.63	20.8
31	7.88	21.4	**94**	9.17	20.7	**179**	9.63	20.8
32	7.86	21.2	**95**	9.17	20.7	**186**	9.64	20.8
33	7.83	21.2	**96**	9.21	20.8	**188**	9.64	20.7
34	8.45	21.1	**97**	9.21	20.7	**191**	9.63	20.7
35	8.44	21	**98**	9.21	20.7	**203**	9.62	20.8
36	8.45	21	**99**	9.21	20.7	**205**	9.62	20.7
37	8.21	21	**100**	9.28	20.7	**207**	9.63	20.8
38	8.14	21	**101**	9.27	20.7	**220**	9.62	20.8
39	8.11	21	**103**	9.27	20.7	**230**	9.62	20.7
40	8.1	20.9	**104**	9.33	20.7	**240**	9.61	20.7
41	8.27	20.9	**105**	9.32	20.7	**250**	9.6	20.6
43	8.23	20.8	**107**	9.33	20.7	**262**	9.6	20.7
44	8.23	20.8	**108**	9.32	20.7	**276**	9.58	20.6
45	8.34	20.7	**110**	9.35	20.6	**290**	9.57	20.7
46	8.31	20.7	**112**	9.35	20.6	**318**	9.56	20.7
48	8.38	20.6	**113**	9.42	20.6	**504**	9.48	21.3
49	8.37	20.6	**114**	9.41	20.6	**506**	9.49	21.3
50	8.37	20.5	**116**	9.42	20.6	**877**	9.38	21.2
51	8.49	20.4	**117**	9.45	20.6	**878**	9.4	21.2
53	8.46	20.4	**119**	9.45	20.6	**880**	9.39	21.2
55	8.52	20.5	**120**	9.46	20.6	**881**	9.38	21.2
56	8.51	20.6	**122**	9.46	20.6	**1550**	9.34	22.7
57	8.62	20.6	**123**	9.47	20.6	**1569**	9.34	22.7

Electronic Annex EA-3: Reactor effluent chemistry

Ion chromatography							
Ash sample #8						Ash sample #7	
Sampling time min.	F mM	Cl mM	SO_4 mM	S_2O_3 mM	SO_3 mM	Sampling time min.	NO_3 mM
1.2	7.1.E-01	2.0.E+00	2.2.E+01	5.4.E-01	Oxidized	0.5	5.3.E-02
4.3	7.2.E-01	3.9.E-01	3.8.E+00	1.4.E-01	Oxidized	1.4	2.7.E-02
9	1.6.E-01	9.0.E-02	5.8.E-01	4.9.E-02	Oxidized	13	6.0.E-04
19.6	5.0.E-02	2.0.E-02	1.1.E-01	2.0.E-02	Oxidized	13.9	5.4.E-04
36.6	2.5.E-02	4.4.E-03	2.6.E-02	9.4.E-03	2.1.E-03	14.8	5.7.E-04
53	1.7.E-02	3.9.E-03	1.2.E-02	7.8.E-03	1.6.E-03	15.8	5.0.E-04
69	1.4.E-02	2.9.E-03	8.2.E-03	6.7.E-03	1.5.E-03	27	2.5.E-04
88	1.2.E-02	4.3.E-03	5.3.E-03	5.9.E-03	1.5.E-03	27.9	1.1.E-04
106	1.1.E-02	3.6.E-03	4.5.E-03	6.3.E-03	1.5.E-03	40	9.9.E-05
123	9.6.E-03	2.9.E-03	4.0.E-03	5.6.E-03	1.4.E-03		
139	9.1.E-03	2.9.E-03	3.7.E-03	5.8.E-03	1.4.E-03		
195	7.0.E-03	1.7.E-03	3.5.E-03	5.1.E-03	1.3.E-03		
280	4.9.E-03	1.3.E-03	2.7.E-03	4.7.E-03	8.6.E-04		
401	3.5.E-03	1.1.E-03	2.4.E-03	3.4.E-03	6.2.E-04		
548	2.5.E-03	1.5.E-03	1.9.E-03	2.9.E-03	5.1.E-04		
1093	1.3.E-03	3.4.E-04	5.9.E-04	1.6.E-03	2.2.E-04		
2821	5.1.E-04	3.5.E-04	3.9.E-04	3.5.E-04	0.0.E+00		
4524	2.5.E-04	3.0.E-04	2.4.E-04	1.2.E-04	0.0.E+00		
5979	0.0.E+00	2.3.E-04	2.6.E-04	0.0.E+00	0.0.E+00		
8934	0.0.E+00	1.7.E-04	2.0.E-04	0.0.E+00	0.0.E+00		
11497	0.0.E+00	1.5.E-04	8.5.E-05	0.0.E+00	0.0.E+00		
Estimated uncertainty (%)	5	5	5	5	NA		5

NA, not available.

Color codes:

Red values were under the limit of quantification.

Gray values were analysed semi-quantitative.

Electronic Annex EA-3: Reactor effluent chemistry

Inductively coupled plasma optical emission spectroscopy, Ash sample #8										
Samp. time	**SiO_2**	**Na**	**K**	**Ca**	**Mg**	**Fe**	**Al**	**Sr**	**Mn**	**Ti**
min.	**mM**	**mM**	**mM**	**mM**	**mM**	**mM**	**mM**	**mM**	**mM**	**mM**
1.2	2.1.E-01	18	1.5.E-01	13	4.1	2.2.E-05	8.0.E-04	1.0.E-02	3.4.E-02	0
4.3	1.2.E-01	3.3	3.9.E-02	2.7	6.3.E-01	3.6.E-05	2.3.E-03	2.1.E-03	5.5.E-03	0
9	1.1.E-01	8.1.E-01	3.7.E-03	5.1.E-01	1.4.E-01	4.3.E-04	3.3.E-03	4.1.E-04	1.0.E-03	8.5.E-05
19.6	1.1.E-01	2.3.E-01	1.0.E-04	1.6.E-01	2.7.E-02	8.4.E-05	5.5.E-03	1.1.E-04	1.5.E-04	0
53	8.6.E-02	7.8.E-02	0	8.8.E-02	5.7.E-03	0	1.3.E-02	4.8.E-05	2.1.E-06	5.6.E-05
106	6.1.E-02	4.6.E-02	0	7.8.E-02	4.5.E-03	1.3.E-04	1.5.E-02	3.8.E-05	1.9.E-06	2.2.E-05
195	4.5.E-02	2.9.E-02	2.4.E-04	6.4.E-02	4.5.E-03	2.1.E-05	1.2.E-02	2.9.E-05	1.1.E-05	2.1.E-06
280	4.0.E-02	2.3.E-02	2.3.E-04	5.3.E-02	4.1.E-03	1.6.E-05	1.1.E-02	2.4.E-05	9.3.E-06	4.0.E-06
401	3.6.E-02	1.8.E-02	5.7.E-04	4.1.E-02	3.6.E-03	1.4.E-05	6.7.E-03	1.9.E-05	1.0.E-05	3.1.E-06
548	3.5.E-02	1.4.E-02	6.0.E-05	3.3.E-02	3.5.E-03	1.8.E-05	7.7.E-03	1.5.E-05	1.1.E-05	5.6.E-06
1093	3.3.E-02	9.4.E-03	6.1.E-06	2.1.E-02	3.9.E-03	1.4.E-05	5.1.E-03	9.8.E-06	7.1.E-06	2.5.E-06
2821	2.8.E-02	7.0.E-03	0	1.2.E-02	5.2.E-03	6.1.E-06	7.1.E-03	7.9.E-06	1.2.E-05	8.8.E-06
4524	1.9.E-02	4.5.E-03	1.1.E-04	7.0.E-03	3.7.E-03	1.1.E-05	2.8.E-03	5.2.E-06	1.7.E-05	2.1.E-06
5979	1.7.E-02	4.2.E-03	0	6.7.E-03	4.0.E-03	7.3.E-06	3.5.E-03	5.6.E-06	2.1.E-05	3.1.E-06
8934	1.4.E-02	3.4.E-03	8.4.E-05	5.9.E-03	3.4.E-03	0	2.8.E-03	5.7.E-06	3.3.E-05	4.2.E-06
11497	1.2.E-02	2.8.E-03	2.4.E-04	4.8.E-03	2.9.E-03	3.6.E-06	2.3.E-03	4.9.E-06	5.2.E-05	4.6.E-06
13082	1.0.E-02	2.3.E-03	1.9.E-04	4.0.E-03	2.4.E-03	7.2.E-07	2.0.E-03	4.2.E-06	7.0.E-05	1.3.E-06
21779	5.5.E-03	6.5.E-03	2.5.E-03	2.9.E-03	1.3.E-03	0	5.1.E-04	3.1.E-06	1.4.E-04	1.3.E-06
Estim. Unc. (%)	3-5	3-5	NA	3-5	3-5	NA	3-5	3-5	3-5	NA

Samp. time	**S (total)**	**P**	**Mo**	**Br**	**B**	**Cr**	**W**	**Ba**	**Sb**	**As**	**V**
min.	**mM**	**mM**	**mM**	**mM**	**mM**	**mM**	**mM**	**mM**	**mM**	**mM**	**mM**
1.2	2.5.E+01	0	4.6.E-04	6.8.E-03	4.3.E-03	0	0	7.0.E-05	0	0	1.2.E-03
4.3	4.4.E+00	0	0	2.5.E-03	0	0	2.5.E-03	1.4.E-05	7.9.E-05	0	8.3.E-04
9	8.0.E-01	2.3.E-03	0	6.7.E-03	0	0	3.8.E-04	1.5.E-06	7.8.E-04	5.7.E-05	3.1.E-04
19.6	1.7.E-01	2.6.E-03	0	0	0	0	0	1.7.E-06	1.7.E-04	0	2.2.E-04
53	2.3.E-02	2.7.E-04	0	0	0	0	0	0	2.3.E-05	9.3.E-06	4.9.E-04
106	1.2.E-02	7.1.E-04	0	0	5.9.E-05	0	0	6.2.E-06	9.1.E-05	0	2.5.E-04
195	1.4.E-02	6.4.E-04	7.6.E-06	1.7.E-04	8.2.E-05	0	0	1.5.E-05	6.6.E-06	0	6.1.E-05
280	1.1.E-02	5.6.E-04	0	3.6.E-04	0	0	0	5.8.E-05	6.1.E-05	0	6.4.E-05
401	8.9.E-03	5.5.E-05	4.0.E-06	0	0	0	8.5.E-05	4.9.E-05	9.9.E-06	0	7.4.E-05
548	7.0.E-03	6.9.E-05	1.1.E-05	6.0.E-06	0	0	7.2.E-06	5.8.E-05	5.1.E-05	6.7.E-07	2.7.E-05
1093	3.2.E-03	0	0	8.9.E-05	0	0	2.3.E-05	0	4.3.E-05	0	4.3.E-05
2821	1.1.E-03	2.6.E-04	0	4.2.E-04	0	3.1.E-06	0	4.6.E-05	2.9.E-05	0	1.6.E-05
4524	7.0.E-04	1.6.E-04	0	0	0	0	0	6.0.E-06	3.0.E-05	0	2.1.E-05
5979	6.0.E-04	6.6.E-05	0	5.9.E-05	0	0	0	5.5.E-06	3.9.E-05	0	7.7.E-06
8934	4.4.E-04	1.1.E-04	0	1.5.E-04	0	0	0	1.2.E-05	5.2.E-05	1.3.E-06	0
11497	2.9.E-04	1.8.E-04	0	6.3.E-05	0	2.9.E-06	8.2.E-05	4.2.E-06	3.6.E-05	8.6.E-05	2.2.E-05
13082	3.6.E-04	0	0	0	0	0	0	3.2.E-06	4.1.E-05	4.9.E-06	3.2.E-05
21779	4.7.E-04	0	4.6.E-06	0	1.8.E-06	5.6.E-06	0	1.5.E-06	7.3.E-05	0	0
Estim. Unc. (%)	3-5	NA	NA	NA	NA	NA	3-5	NA	NA	NA	NA

Electronic Annex EA-3: Reactor effluent chemistry

Inductively coupled plasma sector field mass spectroscopy, Ash sample #8. The concentrations are in mM

Time (min)	Ag	Al	As	Au	B	Ba	Be	Bi	Br	Ca	Cd	Ce	Co	Cr	Cs
1.2	2.7.E-06	3.1.E-03	4.1.E-06	6.1.E-08	3.5.E-03	1.0.E-04	6.2.E-06	1.0.E-08	1.4.E-03	1.4.E+01	5.6.E-06	6.3.E-07	6.4.E-05	3.5.E-06	8.4.E-08
4.3	4.6.E-07	2.2.E-03	3.9.E-06	1.1.E-08	1.3.E-03	1.8.E-05	1.2.E-06	5.4.E-09	2.6.E-04	2.6.E+00	8.4.E-07	1.8.E-07	1.0.E-05	1.5.E-06	1.8.E-08
9	6.5.E-08	2.8.E-03	2.1.E-06	5.9.E-09	5.6.E-04	4.2.E-06	1.8.E-07	3.4.E-09	6.4.E-05	5.1.E-01	1.4.E-07	6.9.E-08	2.0.E-06	1.4.E-06	6.0.E-09
36.5	1.5.E-08	9.7.E-03	4.8.E-06	1.7.E-09	1.5.E-04	5.2.E-07	3.7.E-08	2.9.E-09	3.4.E-06	9.7.E-02	1.9.E-08	2.4.E-08	9.5.E-08	4.7.E-07	1.9.E-09
69	2.9.E-09	1.5.E-02	3.0.E-06	2.3.E-09	7.7.E-05	3.4.E-07	2.6.E-08	8.8.E-10	2.3.E-06	8.5.E-02	3.8.E-09	4.7.E-09	9.1.E-08	8.2.E-06	8.3.E-10
106	1.7.E-09	1.4.E-02	2.0.E-06	1.7.E-09	4.5.E-05	5.8.E-06	3.2.E-08	1.5.E-09	2.1.E-06	8.0.E-02	3.6.E-09	6.9.E-09	3.4.E-08	3.5.E-07	8.3.E-10
139	1.5.E-09	1.3.E-02	2.0.E-06	1.4.E-09	7.5.E-05	2.8.E-07	1.8.E-08	1.1.E-09	1.2.E-06	7.2.E-02	6.8.E-09	1.1.E-08	3.7.E-08	2.1.E-07	7.5.E-10
195	9.5.E-10	9.6.E-03	1.0.E-06	1.0.E-09	1.1.E-04	2.2.E-05	2.1.E-08	5.6.E-10	1.1.E-06	6.0.E-02	8.3.E-09	1.7.E-09	3.6.E-08	1.1.E-06	7.3.E-10
1093	1.9.E-09	4.0.E-03	9.8.E-08	5.7.E-10	2.1.E-05	1.2.E-07	2.1.E-09	4.2.E-10	3.7.E-07	2.0.E-02	1.8.E-09	3.4.E-10	2.6.E-08	3.2.E-07	2.9.E-10
21779	7.8.E-09	4.2.E-04	2.9.E-08	9.8.E-10	2.5.E-06	1.2.E-06	1.4.E-08	9.8.E-10	3.6.E-06	2.8.E-03	4.8.E-08	1.6.E-09	6.6.E-07	2.3.E-07	1.4.E-09
Est. Unc. (%)	NA	10	50	NA	10-50	10-50	50	NA	NA	10	50	50	50	50	NA

Time (min)	Cu	Dy	Er	Eu	Fe	Ga	Gd	Ge	Hf	Hg	Ho	I	Ir	K	La
1.2	7.2.E-04	5.2.E-08	3.0.E-08	1.3.E-08	1.4.E-04	1.1.E-06	6.2.E-08	5.3.E-06	1.3.E-08	1.7.E-07	9.2.E-09	5.6.E-05	3.6.E-10	1.4.E-01	4.8.E-07
4.3	7.2.E-05	1.9.E-08	9.0.E-09	3.1.E-09	4.9.E-04	3.1.E-06	1.9.E-08	1.8.E-06	1.5.E-08	6.1.E-08	3.2.E-09	1.9.E-05	1.1.E-10	2.8.E-02	9.2.E-08
9	1.1.E-05	8.1.E-09	4.5.E-09	2.6.E-09	2.6.E-04	8.6.E-06	9.3.E-09	1.9.E-06	5.3.E-09	3.9.E-08	1.5.E-09	7.2.E-06	0	7.9.E-03	3.1.E-08
36.5	6.1.E-06	2.3.E-09	1.1.E-09	4.8.E-10	6.8.E-05	8.4.E-06	2.7.E-09	1.2.E-06	1.3.E-09	1.1.E-08	4.6.E-10	1.4.E-06	0	1.9.E-03	1.3.E-08
69	1.7.E-06	5.4.E-10	2.2.E-10	2.0.E-10	5.5.E-05	3.8.E-06	1.3.E-09	7.4.E-07	6.3.E-10	9.4.E-09	1.7.E-10	8.4.E-07	3.6.E-11	1.2.E-03	2.6.E-09
106	3.4.E-06	5.0.E-10	2.0.E-10	1.0.E-11	2.7.E-05	2.6.E-06	6.5.E-10	4.6.E-07	5.9.E-10	7.7.E-09	9.2.E-11	6.0.E-07	2.4.E-11	9.4.E-04	3.5.E-09
139	9.5.E-07	8.3.E-10	2.5.E-10	1.4.E-10	2.3.E-05	2.2.E-06	1.0.E-09	4.2.E-07	8.3.E-10	6.4.E-09	9.3.E-11	4.8.E-07	0	8.1.E-04	6.5.E-09
195	7.0.E-07	1.5.E-10	2.6.E-10	1.0.E-11	1.4.E-05	1.6.E-06	4.7.E-10	2.8.E-07	2.8.E-10	5.0.E-09	4.7.E-11	3.1.E-07	0	6.3.E-04	5.3.E-10
1093	5.9.E-07	4.4.E-11	5.0.E-11	1.0.E-10	6.5.E-06	9.4.E-07	1.5.E-10	7.4.E-08	2.4.E-10	7.4.E-09	2.7.E-11	1.7.E-07	1.4.E-11	3.2.E-04	3.5.E-10
21779	2.0.E-05	1.7.E-10	9.6.E-11	4.0.E-11	3.3.E-06	1.1.E-07	9.5.E-10	3.1.E-08	2.2.E-10	9.1.E-10	5.3.E-11	2.2.E-07	1.4.E-11	2.0.E-03	1.0.E-09
Est. Unc. (%)	10-50	NA	NA	NA	10-50	NA	NA	NA	NA	50	NA	NA	NA	10	50

Time (min)	Li	Lu	Mg	Mn	Mo	Na	Nb	Nd	Ni	Os	P	Pb	Pd	Pr	Pt
1.2	1.6.E-02	2.9.E-09	4.4.E+00	3.0.E-02	4.6.E-05	1.9.E+01	3.8.E-08	4.0.E-07	3.0.E-04	1.3.E-07	2.4.E-04	8.9.E-07	4.1.E-07	6.2.E-08	3.4.E-08
4.3	3.7.E-03	1.5.E-09	6.4.E-01	4.9.E-03	1.8.E-05	3.4.E+00	7.2.E-08	8.1.E-08	5.2.E-05	4.0.E-08	1.9.E-04	3.6.E-07	9.5.E-08	1.9.E-08	6.9.E-09
9	1.1.E-03	6.0.E-10	1.4.E-01	8.6.E-04	7.8.E-06	8.5.E-01	2.6.E-08	2.9.E-08	1.2.E-05	2.7.E-08	1.9.E-04	2.1.E-07	2.3.E-08	7.1.E-09	3.1.E-09
36.5	2.0.E-04	1.1.E-10	7.5.E-03	3.4.E-05	1.3.E-06	1.0.E-01	1.2.E-08	1.3.E-08	3.7.E-06	4.3.E-09	8.0.E-04	9.9.E-08	8.4.E-10	2.7.E-09	8.6.E-10
69	1.3.E-04	7.9.E-11	4.6.E-03	1.7.E-05	1.3.E-06	6.0.E-02	1.3.E-08	2.9.E-09	6.1.E-06	2.2.E-09	7.7.E-04	6.6.E-08	3.3.E-10	7.7.E-10	4.3.E-10
106	9.3.E-05	5.3.E-11	4.0.E-03	1.2.E-05	4.5.E-06	4.3.E-02	1.1.E-08	2.7.E-09	9.5.E-06	2.2.E-09	6.7.E-04	8.9.E-08	1.9.E-09	6.8.E-10	1.9.E-10
139	8.5.E-05	7.6.E-11	4.1.E-03	1.1.E-05	4.0.E-07	3.5.E-02	8.6.E-09	4.8.E-09	8.0.E-07	1.7.E-09	6.1.E-04	5.9.E-08	1.4.E-09	1.0.E-09	1.1.E-10
195	6.3.E-05	5.0.E-11	3.9.E-03	9.8.E-06	3.4.E-07	2.9.E-02	3.1.E-09	6.4.E-10	1.4.E-06	9.6.E-10	2.5.E-04	5.0.E-08	3.9.E-11	2.9.E-10	1.5.E-10
1093	3.3.E-05	1.0.E-11	3.4.E-03	8.3.E-06	1.1.E-07	9.3.E-03	1.5.E-09	7.3.E-11	9.6.E-07	2.0.E-10	1.0.E-04	4.3.E-08	0.0.E+00	8.9.E-11	5.0.E-11
21779	1.4.E-07	2.1.E-11	1.2.E-03	1.0.E-04	4.5.E-08	6.7.E-03	5.4.E-10	6.8.E-10	8.1.E-06	6.0.E-10	6.9.E-05	8.9.E-08	1.2.E-09	2.1.E-10	5.1.E-13
Est. Unc. (%)	10-50	NA	10	10-50	50	10	NA	50	10-50	NA	10-50	50	NA	NA	NA

Electronic Annex EA-3: Reactor effluent chemistry

Inductively coupled plasma sector field mass spectroscopy, Ash sample #8															
Sampl. time min.	Rb mM	Re mM	Rh mM	Ru mM	S mM	Sb mM	Sc mM	Se mM	Si mM	Sm mM	Sn mM	Sr mM	Ta mM	Tb mM	Te mM
1.2	4.5.E-05	4.8.E-06	3.5.E-08	1.7.E-07	2.9.E+01	7.3.E-07	5.2.E-06	5.5.E-04	1.9.E-01	7.1.E-08	2.2.E-06	9.3.E-03	1.6.E-08	1.4.E-08	1.7.E-08
4.3	9.3.E-06	1.1.E-06	8.1.E-09	6.5.E-08	4.8.E+00	3.5.E-07	5.2.E-07	2.0.E-04	1.2.E-01	2.2.E-08	1.2.E-06	1.8.E-03	1.3.E-08	3.4.E-09	1.5.E-08
9	3.0.E-06	2.6.E-07	1.7.E-09	1.7.E-08	8.6.E-01	2.1.E-07	1.3.E-07	1.6.E-04	1.2.E-01	9.0.E-09	8.1.E-07	4.0.E-04	1.6.E-09	1.5.E-09	6.0.E-08
36.5	7.5.E-07	1.3.E-08	2.3.E-10	2.4.E-09	4.7.E-02	3.3.E-07	3.6.E-08	1.0.E-04	1.1.E-01	2.6.E-09	1.2.E-06	5.3.E-05	3.4.E-10	4.9.E-10	1.1.E-07
69	4.7.E-07	9.5.E-09	9.7.E-11	4.4.E-10	2.1.E-02	9.0.E-08	1.6.E-08	3.7.E-05	8.3.E-02	5.8.E-10	5.6.E-07	4.2.E-05	1.3.E-09	2.0.E-10	9.4.E-08
106	3.8.E-07	6.3.E-09	1.9.E-10	7.4.E-09	1.5.E-02	5.9.E-08	5.5.E-09	1.8.E-05	6.7.E-02	1.0.E-09	5.6.E-07	3.7.E-05	1.4.E-11	1.1.E-10	7.9.E-08
139	3.4.E-07	5.5.E-09	9.0.E-11	1.4.E-09	1.4.E-02	3.5.E-08	1.1.E-08	1.7.E-05	6.0.E-02	1.1.E-09	5.0.E-07	3.4.E-05	2.1.E-09	1.2.E-10	7.3.E-08
195	2.8.E-07	3.7.E-09	9.7.E-11	2.0.E-09	1.2.E-02	3.7.E-08	7.3.E-09	1.1.E-05	4.8.E-02	3.9.E-10	2.2.E-07	2.7.E-05	2.7.E-09	6.9.E-12	4.8.E-08
1093	1.5.E-07	1.3.E-09	8.6.E-11	0.0.E+00	2.9.E-03	1.6.E-08	5.1.E-09	2.1.E-06	3.6.E-02	1.1.E-10	6.7.E-08	9.0.E-06	2.2.E-09	0.0.E+00	1.1.E-08
21779	7.3.E-07	9.6.E-11	7.6.E-11	1.6.E-09	4.9.E-04	1.4.E-08	3.5.E-09	0.0.E+00	5.8.E-03	1.3.E-10	3.2.E-07	3.4.E-06	2.0.E-09	1.8.E-11	9.7.E-10
Estim. Unc. (%)	NA	NA	NA	NA	10	NA	NA	NA	10	NA	50	10-50	NA	NA	NA

Sampl. time min.	Th mM	Ti mM	Tl mM	Tm mM	U mM	W mM	V mM	Y mM	Yb mM	Zn mM	Zr mM
1.2	7.8.E-09	3.2.E-05	3.1.E-08	3.7.E-09	7.4.E-08	2.2.E-07	1.2.E-05	1.0.E-06	2.2.E-08	1.8.E-03	1.1.E-06
4.3	8.5.E-09	1.1.E-04	6.5.E-09	2.1.E-09	3.3.E-08	2.5.E-07	1.7.E-05	2.1.E-07	8.8.E-09	4.3.E-04	1.2.E-06
9	3.5.E-09	5.0.E-05	2.4.E-09	6.8.E-10	1.4.E-08	2.3.E-07	3.3.E-05	7.2.E-08	4.5.E-09	1.0.E-04	5.0.E-07
36.5	1.2.E-09	9.4.E-06	4.9.E-10	1.8.E-10	7.6.E-09	6.5.E-08	2.5.E-04	2.1.E-08	1.3.E-09	5.0.E-05	7.9.E-08
69	1.2.E-10	3.1.E-06	4.8.E-10	6.5.E-11	5.2.E-09	4.6.E-08	1.8.E-04	7.4.E-09	3.1.E-10	1.7.E-05	4.9.E-08
106	1.5.E-10	1.9.E-06	4.9.E-10	3.9.E-11	4.4.E-09	3.4.E-08	1.0.E-04	6.8.E-09	3.6.E-10	3.1.E-05	3.4.E-08
139	6.4.E-10	2.0.E-06	3.4.E-10	1.7.E-10	3.9.E-09	2.5.E-08	8.2.E-05	7.1.E-09	1.3.E-10	1.1.E-05	2.6.E-08
195	7.4.E-11	1.2.E-06	3.2.E-10	2.6.E-11	2.2.E-09	2.2.E-08	5.7.E-05	1.4.E-09	1.2.E-10	1.3.E-05	1.1.E-08
1093	5.1.E-11	4.4.E-07	8.5.E-11	9.5.E-12	4.7.E-10	9.0.E-09	2.1.E-05	4.4.E-10	2.4.E-10	6.7.E-06	3.4.E-09
21779	8.4.E-11	4.6.E-07	5.2.E-10	0.0.E+00	3.3.E-10	2.6.E-09	1.6.E-06	1.2.E-09	7.3.E-11	6.5.E-05	1.4.E-08
Estim. Unc. (%)	NA	10-50	NA	NA	50	NA	10-50	NA	NA	10-50	NA

Electronic Annex EA-4: Grain size distribution

	Ash sample #1			Ash sample #6			Ash sample #8		
Grain Size (µm)	Cumul. Mass (%)	Mass (%)	Std dev. (%)	Cumul. Mass	Mass	Std dev.	Cumul. Mass	Mass	Std dev.
350	100		0	100		0	100		0
294	100	0	0	100	0	0	100	0	0
246	100	0	0	100	0	0	100	0	0
206	100	0	0	99.74	0.26	0.26	100	0	0
174	100	0	0	98.95	0.79	1	100	0	0
146	100	0	0	95.85	3.1	1.45	99.1	0.9	0.1
122	98.78	1.22	0.44	89.45	6.4	1.61	97.02	2.08	0.24
102	95.16	3.62	0.61	80.05	9.4	1.26	92.56	4.46	0.33
86	87.27	7.89	0.54	69.83	10.22	0.85	85.61	6.95	0.31
72	74.45	12.82	0.37	59.38	10.45	0.54	76.19	9.42	0.22
60	59.25	15.2	0.17	49.71	9.67	0.36	65.44	10.75	0.12
50	45.18	14.07	0.17	41.4	8.31	0.28	54.93	10.51	0.05
42	34.1	11.08	0.33	34.67	6.73	0.26	45.9	9.03	0.02
36	26.57	7.53	0.52	29.57	5.1	0.24	38.98	6.92	0.04
30	20.21	6.36	0.65	24.45	5.12	0.21	32.05	6.93	0.04
25	15.92	4.29	0.64	20.24	4.21	0.15	26.35	5.7	0.02
21	13.03	2.89	0.57	16.95	3.29	0.09	21.88	4.47	0.02
18	11.1	1.93	0.52	14.56	2.39	0.05	18.59	3.29	0.03
15	9.3	1.8	0.49	12.24	2.32	0.02	15.38	3.21	0.04
12	7.62	1.68	0.44	9.97	2.27	0.02	12.27	3.11	0.04
10	6.52	1.1	0.4	8.46	1.51	0.03	10.27	2	0.04
8.6	5.75	0.77	0.36	7.4	1.06	0.03	8.9	1.37	0.04
7.4	5.07	0.68	0.33	6.48	0.92	0.03	7.74	1.16	0.03
6.2	4.36	0.71	0.3	5.53	0.95	0.03	6.56	1.18	0.03
5.2	3.72	0.64	0.27	4.7	0.83	0.03	5.57	0.99	0.03
4.4	3.18	0.54	0.25	4.01	0.69	0.04	4.75	0.82	0.03
3.6	2.61	0.57	0.23	3.28	0.73	0.04	3.89	0.86	0.04
3	2.16	0.45	0.21	2.71	0.57	0.04	3.22	0.67	0.04
2.6	1.84	0.32	0.2	2.31	0.4	0.04	2.75	0.47	0.03
2.2	1.52	0.32	0.18	1.91	0.4	0.04	2.27	0.48	0.03
1.8	1.18	0.34	0.15	1.48	0.43	0.03	1.77	0.5	0.03

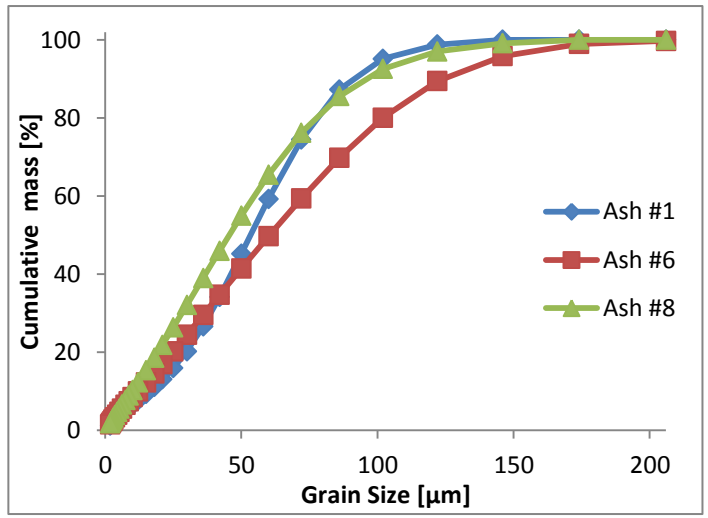

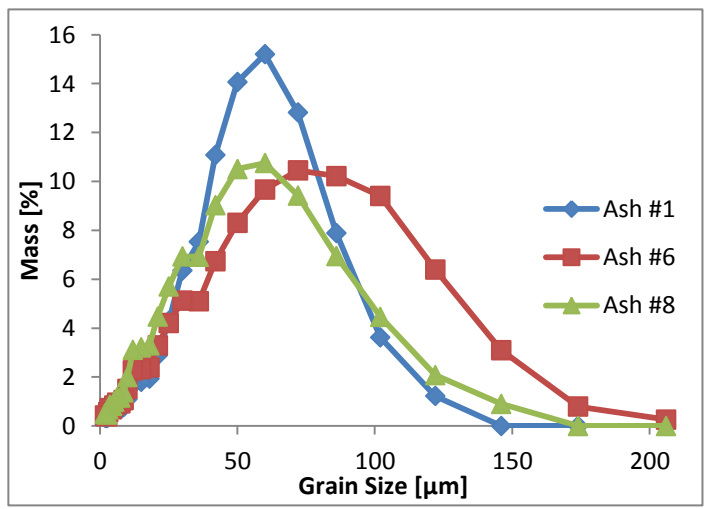

Electronic Annex EA-5: XPS data

At%	Ash sample #1		Ash sample #7		Ash sample #8	
	Fresh	Pure water exposed*	Fresh	Pure water exposed*	Fresh	Pure water exposed*
O	54.9	62.0	57.5	59.1	56.7	59.4
Si	23.1	22.4	24.6	23.3	23.8	24.3
Al	6.2	7.1	6.4	7.8	6.3	7.6
Fe	3.3	4.2	2.3	5.1	2.3	3.5
Ca	3.4	1.7	3.1	1.9	3.1	2.2
Mg	2.5	1.2	2.3	1.3	2.6	1.5
Na	2.4	0.5	2.3	0.5	2.3	0.6
Ti	0.5	1.0	0.5	1.1	0.5	0.9
S	3.1	<0,5%	0.8	<0,5%	2.0	<0,5%
F	0.7	BDL	<0,5%	BDL	<0,5%	BDL
Cl	BDL	BDL	BDL	BDL	<0,5%	BDL
C	Excluded	Excluded	Excluded	Excluded	Excluded	Excluded

BDL, below detection limit.

*Ash sample #8 was exposed to water in a single pass flow-through reactor for 15 days, while Ash sample #1 and #7 were exposed for 4 weeks.

Electronic Annex EA-6: Element fluxes

Elem.	10 min µmol/g	1 hour µmol/g	8 hours µmol/g	15 days µmol/g
Ag	5.7.E-07	-	-	-
Al	2.2.E-03	3.9.E-02	3.5.E-01	2.0
As	0.0.E+00	1.9.E-05	3.4.E-05	-
Au	BDL	-	-	-
B	1.1.E-03	-	-	-
Ba	2.3.E-05	-	-	-
Be	1.3.E-06	-	-	-
Bi	BDL	-	-	-
Br	3.2.E-04	-	-	-
Ca	3.1.E+00	3.6.E+00	5.4	16
Cd	1.2.E-06	1.3.E-06	-	-
Ce	1.8.E-07	2.7.E-07	-	-
Cl	4.6.E-01	5.0.E-01	5.4.E-01	-
Co	1.4.E-05	1.6.E-05	1.6.E-05	-
Cr	1.5.E-06	9.0.E-06	1.9.E-05	4.6.E-04
Cs	BDL	-	-	-
Cu	1.4.E-04	1.6.E-04	1.7.E-04	-
Dy	BDL	-	-	-
Er	BDL	-	-	-
Eu	BDL	-	-	-
F	3.8.E-01	5.2.E-01	7.2.E-01	8.5.E-01
Fe	2.7.E-04	6.7.E-04	9.6.E-04	-
Ga	4.4.E-06	3.5.E-05	9.8.E-05	4.9.E-04
Gd	BDL	-	-	-
Ge	2.1.E-06	7.0.E-06	-	-
Hf	BDL	-	-	-
Hg	6.0.E-08	-	-	-
Ho	BDL	-	-	-
I	1.7.E-05	-	-	-
Ir	BDL	-	-	-
K	3.2.E-02	4.4.E-02	6.9.E-02	2.2
La	1.1.E-07	-	-	-
Li	4.0.E-03	5.4.E-03	7.7.E-03	8.7.E-03
Lu	BDL	-	-	-
Mg	9.1.E-01	9.8.E-01	1.1	4.3
Mn	6.4.E-03	6.7.E-03	7.1.E-03	0.1
Mo	1.6.E-05	2.6.E-05	3.5.E-05	-
Na	4.3.E+00	4.9.E+00	5.8	19

Elem.	10 min µmol/g	1 hour µmol/g	8 hours µmol/g	15 days µmol/g
Nb	BDL	-	-	-
Nd	9.6.E-08	-	-	-
Ni	6.7.E-05	9.0.E-05	1.5.E-04	7.9.E-03
NO3	4.8.E-03	5.1.E-03	-	-
Os	4.2.E-08	-	-	-
P	1.7.E-04	2.9.E-03	1.6.E-02	1.6.E-01
Pb	3.2.E-07	7.8.E-07	1.5.E-06	-
Pd	1.0.E-07	-	-	-
Pr	BDL	-	-	-
Pt	BDL	-	-	-
Rb	1.1.E-05	1.5.E-05	-	-
Re	1.2.E-06	1.4.E-06	-	-
Rh	BDL	-	-	-
Ru	BDL	-	-	-
S (total)	6.1.E+00	6.5.E+00	6.9.E+00	7.0.E+00
S2O3	1.4.E-01	1.9.E-01	3.5.E-01	5.1.E-01
Sb	3.0.E-07	1.1.E-06	-	-
Sc	1.0.E-06	-	-	-
Se	2.1.E-04	6.2.E-04	1.0.E-03	1.2.E-03
Si	1.1.E-01	5.2.E-01	2.3.E+00	2.1.E+01
Sm	BDL	-	-	-
Sn	1.0.E-06	5.0.E-06	8.8.E-06	-
SO4	4.8.E+00	5.0.E+00	5.1.E+00	5.3.E+00
Sr	2.1.E-03	2.4.E-03	3.3.E-03	1.2.E-02
Ta	BDL	-	-	-
Tb	BDL	-	-	-
Te	BDL	-	-	-
Th	BDL	-	-	-
Ti	5.7.E-05	1.2.E-04	1.5.E-04	-
Tl	BDL	-	-	-
Tm	BDL	-	-	-
U	2.6.E-08	-	-	-
W	2.0.E-07	5.7.E-07	8.2.E-07	-
V	1.9.E-05	8.1.E-04	3.0.E-03	4.3.E-03
Y	2.5.E-07	-	-	-
Yb	BDL	-	-	-
Zn	4.5.E-04	6.7.E-04	1.1.E-03	5.6.E-02
Zr	7.3.E-07	1.3.E-06	-	-

BDL, below detection limit.

Color codes:

Gray values were analysed semi-quantitative.

Highlighted values were interpolated data based on the calculated release rates.

Electronic Annex EA-7: Release rates

Ion chromatography							
Ash sample #8						Ash sample #7	
Sampling time (min)	F pmol/m2/s	Cl pmol/m2/s	SO_4 pmol/m2/s	S_2O_3 pmol/m2/s	SO_3 pmol/m2/s	Sampling time (min)	NO_3 pmol/m2/s
1.2	1.1.E+03	3.1.E+03	3.5.E+04	8.4.E+02	Oxidized	**0.5**	1.0.E+02
4.3	1.4.E+03	7.6.E+02	7.3.E+03	2.7.E+02	Oxidized	**1.4**	5.1.E+01
9	3.2.E+02	1.8.E+02	1.1.E+03	9.7.E+01	Oxidized	**13**	1.2.E+00
19.6	1.0.E+02	4.0.E+01	2.2.E+02	4.0.E+01	Oxidized	**13.9**	1.0.E+00
36.6	5.1.E+01	8.8.E+00	5.3.E+01	1.9.E+01	4.1.E+00	**14.8**	1.1.E+00
53	3.4.E+01	7.7.E+00	2.3.E+01	1.5.E+01	3.2.E+00	**15.8**	9.7.E-01
69	2.8.E+01	5.8.E+00	1.6.E+01	1.3.E+01	3.0.E+00	**27**	4.8.E-01
88	1.9.E+01	6.7.E+00	8.3.E+00	9.3.E+00	2.3.E+00	**27.9**	2.1.E-01
106	2.2.E+01	7.3.E+00	9.2.E+00	1.3.E+01	3.0.E+00	**40**	1.9.E-01
123	1.9.E+01	5.8.E+00	8.0.E+00	1.1.E+01	2.9.E+00		
139	1.8.E+01	5.7.E+00	7.3.E+00	1.2.E+01	2.8.E+00		
195	1.4.E+01	3.3.E+00	7.0.E+00	1.0.E+01	2.6.E+00		
280	9.4.E+00	2.5.E+00	5.3.E+00	9.1.E+00	1.7.E+00		
401	8.1.E+00	2.5.E+00	5.4.E+00	7.9.E+00	1.4.E+00		
548	5.6.E+00	3.4.E+00	4.2.E+00	6.5.E+00	1.1.E+00		
1093	2.5.E+00	6.9.E-01	1.2.E+00	3.3.E+00	4.5.E-01		
2821	1.0.E+00	6.9.E-01	7.6.E-01	7.0.E-01	0.0.E+00		
4524	4.9.E-01	5.7.E-01	4.7.E-01	2.3.E-01	0.0.E+00		
5979	0.0.E+00	4.2.E-01	4.7.E-01	0.0.E+00	0.0.E+00		
8934	0.0.E+00	3.2.E-01	3.7.E-01	0.0.E+00	0.0.E+00		
11497	0.0.E+00	2.9.E-01	1.7.E-01	0.0.E+00	0.0.E+00		
Estim. Unc. (%)	5	5	5	5	NA		5

NA, not available.

Color codes:

Red values were under the limit of quantification.

Gray values were analysed semi-quantitative.

Electronic Annex EA-7: Release rates

Inductively coupled plasma optical emission spectroscopy, Ash sample #8

Sampling time (min)	SiO2 (pmol/m2/s)	Na (pmol/m2/s)	K (pmol/m2/s)	Ca (pmol/m2/s)	Mg (pmol/m2/s)	Fe (pmol/m2/s)	Al (pmol/m2/s)	Sr (pmol/m2/s)	Mn (pmol/m2/s)	Ti (pmol/m2/s)	S (total) (pmol/m2/s)
1.2	3.3.E+02	2.8.E+04	2.4.E+02	2.0.E+04	6.4.E+03	3.4.E-02	1.3.E+00	1.5.E+01	5.3.E+01	0.0.E+00	3.9.E+04
4.3	2.3.E+02	6.4.E+03	7.5.E+01	5.2.E+03	1.2.E+03	6.8.E-02	4.5.E+00	4.0.E+00	1.1.E+01	0.0.E+00	8.4.E+03
9	2.1.E+02	1.6.E+03	7.4.E+00	1.0.E+03	2.7.E+02	8.4.E-01	6.5.E+00	8.0.E-01	2.1.E+00	1.7.E-01	1.6.E+03
19.6	2.2.E+02	4.7.E+02	2.1.E-01	3.3.E+02	5.5.E+01	1.7.E-01	1.1.E+01	2.2.E-01	3.1.E-01	0.0.E+00	3.4.E+02
53	1.7.E+02	1.5.E+02	0.0.E+00	1.7.E+02	1.1.E+01	0.0.E+00	2.6.E+01	9.4.E-02	4.2.E-03	1.1.E-01	4.4.E+01
106	1.2.E+02	9.4.E+01	0.0.E+00	1.6.E+02	9.2.E+00	2.7.E-01	3.0.E+01	7.6.E-02	3.9.E-03	4.5.E-02	2.4.E+01
195	9.1.E+01	5.8.E+01	4.8.E-01	1.3.E+02	9.0.E+00	4.2.E-02	2.4.E+01	5.8.E-02	2.2.E-02	4.2.E-03	2.7.E+01
280	7.7.E+01	4.3.E+01	4.5.E-01	1.0.E+02	7.9.E+00	3.2.E-02	2.1.E+01	4.6.E-02	1.8.E-02	7.7.E-03	2.2.E+01
401	8.3.E+01	4.0.E+01	1.3.E+00	9.3.E+01	8.3.E+00	3.2.E-02	1.5.E+01	4.3.E-02	2.4.E-02	7.2.E-03	2.0.E+01
548	7.8.E+01	3.2.E+01	1.3.E-01	7.2.E+01	7.8.E+00	4.0.E-02	1.7.E+01	3.4.E-02	2.5.E-02	1.2.E-02	1.6.E+01
1093	6.7.E+01	1.9.E+01	1.2.E-02	4.2.E+01	7.8.E+00	2.8.E-02	1.0.E+01	2.0.E-02	1.4.E-02	5.0.E-03	6.5.E+00
2821	5.5.E+01	1.4.E+01	0.0.E+00	2.3.E+01	1.0.E+01	1.2.E-02	1.4.E+01	1.6.E-02	2.4.E-02	1.7.E-02	2.2.E+00
4524	3.7.E+01	8.7.E+00	2.1.E-01	1.3.E+01	7.2.E+00	2.1.E-02	5.3.E+00	1.0.E-02	3.4.E-02	4.0.E-03	1.4.E+00
5979	3.2.E+01	7.5.E+00	0.0.E+00	1.2.E+01	7.1.E+00	1.3.E-02	6.3.E+00	1.0.E-02	3.9.E-02	5.6.E-03	1.1.E+00
8934	2.7.E+01	6.5.E+00	1.6.E-01	1.1.E+01	6.5.E+00	0.0.E+00	5.3.E+00	1.1.E-02	6.2.E-02	7.9.E-03	8.4.E-01
11497	2.4.E+01	5.6.E+00	4.8.E-01	9.7.E+00	5.9.E+00	7.2.E-03	4.7.E+00	9.9.E-03	1.1.E-01	9.3.E-03	5.9.E-01
13082	2.0.E+01	4.6.E+00	3.7.E-01	7.7.E+00	4.6.E+00	1.4.E-03	3.9.E+00	8.2.E-03	1.4.E-01	2.4.E-03	7.1.E-01
21779	1.1.E+01	1.3.E+01	4.8.E+00	5.5.E+00	2.6.E+00	0.0.E+00	9.9.E-01	5.9.E-03	2.6.E-01	2.4.E-03	9.1.E-01
Estim. Unc. (%)	3-5	3-5	NA	3-5	3-5	NA	3-5	3-5	3-5	NA	3-5

Electronic Annex EA-7: Release rates

Inductively coupled plasma optical emission spectroscopy, Ash sample #8

Sampling time (min)	P (pmol/m2/s)	Mo (pmol/m2/s)	Br (pmol/m2/s)	B (pmol/m2/s)	Cr (pmol/m2/s)	W (pmol/m2/s)	Ba (pmol/m2/s)	Sb (pmol/m2/s)	As (pmol/m2/s)	V (pmol/m2/s)
1.2	0.0.E+00	7.2.E-01	1.1.E+01	6.8.E+00	0.0.E+00	0.0.E+00	1.1.E-01	0.0.E+00	0.0.E+00	1.9.E+00
4.3	0.0.E+00	0.0.E+00	4.8.E+00	0.0.E+00	0.0.E+00	4.9.E+00	2.8.E-02	1.5.E-01	0.0.E+00	1.6.E+00
9	4.6.E+00	0.0.E+00	1.3.E+01	0.0.E+00	0.0.E+00	7.5.E-01	2.9.E-03	1.5.E+00	1.1.E-01	6.2.E-01
19.6	5.2.E+00	0.0.E+00	0.0.E+00	0.0.E+00	0.0.E+00	0.0.E+00	3.5.E-03	3.3.E-01	0.0.E+00	4.3.E-01
53	5.3.E-01	0.0.E+00	0.0.E+00	0.0.E+00	0.0.E+00	0.0.E+00	0.0.E+00	4.5.E-02	1.8.E-02	9.7.E-01
106	1.5.E+00	0.0.E+00	0.0.E+00	1.2.E-01	0.0.E+00	0.0.E+00	1.3.E-02	1.8.E-01	0.0.E+00	5.1.E-01
195	1.3.E+00	1.5.E-02	3.4.E-01	1.6.E-01	0.0.E+00	0.0.E+00	3.0.E-02	1.3.E-02	0.0.E+00	1.2.E-01
280	1.1.E+00	0.0.E+00	7.0.E-01	0.0.E+00	0.0.E+00	0.0.E+00	1.1.E-01	1.2.E-01	0.0.E+00	1.2.E-01
401	1.3.E-01	9.1.E-03	0.0.E+00	0.0.E+00	0.0.E+00	1.9.E-01	1.1.E-01	2.3.E-02	0.0.E+00	1.7.E-01
548	1.5.E-01	2.4.E-02	1.3.E-02	0.0.E+00	0.0.E+00	1.6.E-02	1.3.E-01	1.1.E-01	1.5.E-03	5.9.E-02
1093	0.0.E+00	0.0.E+00	1.8.E-01	0.0.E+00	0.0.E+00	4.7.E-02	0.0.E+00	8.7.E-02	0.0.E+00	8.6.E-02
2821	5.0.E-01	0.0.E+00	8.3.E-01	0.0.E+00	6.1.E-03	0.0.E+00	9.1.E-02	5.8.E-02	0.0.E+00	3.2.E-02
4524	3.1.E-01	0.0.E+00	0.0.E+00	0.0.E+00	0.0.E+00	0.0.E+00	1.2.E-02	5.8.E-02	0.0.E+00	4.0.E-02
5979	1.2.E-01	0.0.E+00	1.1.E-01	0.0.E+00	0.0.E+00	0.0.E+00	1.0.E-02	7.1.E-02	0.0.E+00	1.4.E-02
8934	2.2.E-01	0.0.E+00	2.9.E-01	0.0.E+00	0.0.E+00	0.0.E+00	2.2.E-02	9.9.E-02	2.5.E-03	0.0.E+00
11497	3.7.E-01	0.0.E+00	1.3.E-01	0.0.E+00	5.8.E-03	1.7.E-01	8.5.E-03	7.2.E-02	1.7.E-01	4.5.E-02
13082	0.0.E+00	0.0.E+00	0.0.E+00	0.0.E+00	0.0.E+00	0.0.E+00	6.2.E-03	7.9.E-02	9.6.E-03	6.1.E-02
21779	0.0.E+00	8.8.E-03	0.0.E+00	3.6.E-03	1.1.E-02	0.0.E+00	2.9.E-03	1.4.E-01	0.0.E+00	0.0.E+00
Estim. Unc. (%)	NA	NA	NA	NA	NA	3-5	NA	NA	NA	NA

Electronic Annex EA-7: Release rates

Inductively coupled plasma sector field mass spectroscopy, Ash sample #8. The units of the release rates are pmol/m^2/s													
Time (min.)	**Ag**	**Al**	**As**	**Au**	**B**	**Ba**	**Be**	**Bi**	**Br**	**Ca**	**Cd**	**Ce**	**Co**
1.22	4.1.E-03	4.8.E+00	6.4.E-03	9.4.E-05	5.4.E+00	1.6.E-01	9.6.E-03	1.6.E-05	2.2.E+00	2.1.E+04	8.8.E-03	9.8.E-04	1.0.E-01
4.34	9.0.E-04	4.2.E+00	7.6.E-03	2.2.E-05	2.5.E+00	3.4.E-02	2.3.E-03	1.0.E-05	5.0.E-01	5.1.E+03	1.6.E-03	3.4.E-04	2.0.E-02
9	1.3.E-04	5.6.E+00	4.1.E-03	1.2.E-05	1.1.E+00	8.2.E-03	3.5.E-04	6.8.E-06	1.3.E-01	1.0.E+03	2.8.E-04	1.4.E-04	4.1.E-03
36.5	2.9.E-05	1.9.E+01	9.7.E-03	3.5.E-06	3.0.E-01	1.0.E-03	7.5.E-05	5.8.E-06	6.9.E-03	2.0.E+02	3.8.E-05	4.8.E-05	1.9.E-04
69	5.8.E-06	2.9.E+01	6.1.E-03	4.7.E-06	1.6.E-01	6.9.E-04	5.2.E-05	1.8.E-06	4.6.E-03	1.7.E+02	7.7.E-06	9.4.E-06	1.8.E-04
106	3.4.E-06	3.0.E+01	4.1.E-03	3.5.E-06	9.2.E-02	1.2.E-02	6.4.E-05	3.0.E-06	4.3.E-03	1.6.E+02	7.2.E-06	1.4.E-05	7.0.E-05
139	2.9.E-06	2.6.E+01	3.9.E-03	2.7.E-06	1.5.E-01	5.6.E-04	3.5.E-05	2.2.E-06	2.3.E-03	1.4.E+02	1.3.E-05	2.3.E-05	7.3.E-05
195	1.9.E-06	1.9.E+01	2.0.E-03	2.1.E-06	2.2.E-01	4.5.E-02	4.2.E-05	1.1.E-06	2.1.E-03	1.2.E+02	1.7.E-05	3.5.E-06	7.2.E-05
1093	3.7.E-06	8.0.E+00	2.0.E-04	1.2.E-06	4.3.E-02	2.4.E-04	4.3.E-06	8.4.E-07	7.4.E-04	4.0.E+01	3.6.E-06	6.8.E-07	5.3.E-05
21779	1.5.E-05	8.1.E-01	5.6.E-05	1.9.E-06	4.9.E-03	2.2.E-03	2.7.E-05	1.9.E-06	6.9.E-03	5.5.E+00	9.2.E-05	3.0.E-06	1.3.E-03
Estim. Unc. (%)	NA	10	50	NA	10-50	10-50	50	NA	NA	10	50	50	50
Time (min.)	**Cr**	**Cs**	**Cu**	**Dy**	**Er**	**Eu**	**Fe**	**Ga**	**Gd**	**Ge**	**Hf**	**Hg**	**Ho**
1.22	5.4.E-03	1.3.E-04	1.1.E+00	8.1.E-05	4.7.E-05	1.9.E-05	2.2.E-01	1.7.E-03	9.7.E-05	8.3.E-03	2.0.E-05	2.7.E-04	1.4.E-05
4.34	3.0.E-03	3.4.E-05	1.4.E-01	3.7.E-05	1.7.E-05	6.0.E-06	9.4.E-01	5.9.E-03	3.6.E-05	3.4.E-03	2.9.E-05	1.2.E-04	6.2.E-06
9	2.9.E-03	1.2.E-05	2.2.E-02	1.6.E-05	8.8.E-06	5.1.E-06	5.2.E-01	1.7.E-02	1.8.E-05	3.7.E-03	1.0.E-05	7.7.E-05	3.0.E-06
36.5	9.5.E-04	3.8.E-06	1.2.E-02	4.6.E-06	2.2.E-06	9.6.E-07	1.4.E-01	1.7.E-02	5.4.E-06	2.4.E-03	2.5.E-06	2.2.E-05	9.2.E-07
69	1.6.E-02	1.7.E-06	3.4.E-03	1.1.E-06	4.5.E-07	4.0.E-07	1.1.E-01	7.7.E-03	2.6.E-06	1.5.E-03	1.3.E-06	1.9.E-05	3.3.E-07
106	7.1.E-04	1.7.E-06	6.9.E-03	1.0.E-06	4.0.E-07	2.0.E-08	5.5.E-02	5.3.E-03	1.3.E-06	9.4.E-04	1.2.E-06	1.6.E-05	1.9.E-07
139	4.2.E-04	1.5.E-06	1.9.E-03	1.6.E-06	5.0.E-07	2.8.E-07	4.5.E-02	4.4.E-03	2.0.E-06	8.2.E-04	1.7.E-06	1.3.E-05	1.8.E-07
195	2.1.E-03	1.5.E-06	1.4.E-03	3.1.E-07	5.2.E-07	2.0.E-08	2.8.E-02	3.2.E-03	9.4.E-07	5.6.E-04	5.6.E-07	9.9.E-06	9.4.E-08
1093	6.4.E-04	5.8.E-07	1.2.E-03	8.8.E-08	1.0.E-07	2.1.E-07	1.3.E-02	1.9.E-03	2.9.E-07	1.5.E-04	4.7.E-07	1.5.E-05	5.4.E-08
21779	4.4.E-04	2.6.E-06	3.8.E-02	3.2.E-07	1.8.E-07	7.7.E-08	6.4.E-03	2.1.E-04	1.8.E-06	5.9.E-05	4.3.E-07	1.8.E-06	1.0.E-07
Estim. Unc. (%)	50	NA	10-50	NA	NA	NA	10-50	NA	NA	NA	NA	50	NA
Time (min.)	**I**	**Ir**	**K**	**La**	**Li**	**Lu**	**Mg**	**Mn**	**Mo**	**Na**	**Nb**	**Nd**	**Ni**
1.22	8.8.E-02	5.7.E-07	2.1.E+02	7.5.E-04	2.5.E+01	4.5.E-06	6.8.E+03	4.6.E+01	7.2.E-02	3.0.E+04	6.0.E-05	6.2.E-04	4.7.E-01
4.34	3.7.E-02	2.2.E-07	5.3.E+01	1.8.E-04	7.1.E+00	2.8.E-06	1.2.E+03	9.5.E+00	3.5.E-02	6.5.E+03	1.4.E-04	1.6.E-04	1.0.E-01
9	1.4.E-02	0.0.E+00	1.6.E+01	6.1.E-05	2.2.E+00	1.2.E-06	2.7.E+02	1.7.E+00	1.6.E-02	1.7.E+03	5.2.E-05	5.7.E-05	2.5.E-02
36.5	2.7.E-03	0.0.E+00	3.7.E+00	2.5.E-05	4.1.E-01	2.3.E-07	1.5.E+01	6.9.E-02	2.7.E-03	2.1.E+02	2.4.E-05	2.6.E-05	7.4.E-03
69	1.7.E-03	7.2.E-08	2.4.E+00	5.2.E-06	2.5.E-01	1.6.E-07	9.3.E+00	3.5.E-02	2.6.E-03	1.2.E+02	2.7.E-05	5.9.E-06	1.2.E-02
106	1.2.E-03	4.9.E-08	1.9.E+00	7.1.E-06	1.9.E-01	1.1.E-07	8.2.E+00	2.4.E-02	9.1.E-03	8.7.E+01	2.2.E-05	5.6.E-06	1.9.E-02
139	9.5.E-04	0.0.E+00	1.6.E+00	1.3.E-05	1.7.E-01	1.5.E-07	8.1.E+00	2.1.E-02	7.9.E-04	7.0.E+01	1.7.E-05	9.4.E-06	1.6.E-03
195	6.2.E-04	0.0.E+00	1.3.E+00	1.1.E-06	1.3.E-01	1.0.E-07	7.9.E+00	2.0.E-02	6.7.E-04	5.7.E+01	6.2.E-06	1.3.E-06	2.8.E-03
1093	3.3.E-04	2.8.E-08	6.4.E-01	7.1.E-07	6.6.E-02	2.1.E-08	6.8.E+00	1.7.E-02	2.2.E-04	1.9.E+01	3.0.E-06	1.5.E-07	1.9.E-03
21779	4.3.E-04	2.7.E-08	3.8.E+00	1.9.E-06	2.8.E-04	4.1.E-08	2.3.E+00	2.0.E-01	8.7.E-05	1.3.E+01	1.0.E-06	1.3.E-06	1.6.E-02
Estim. Unc. (%)	NA	NA	10	50	10-50	NA	10	10-50	50	10	NA	50	10-50

Electronic Annex EA-7: Release rates

Time (min.)	Os	P	Pb	Pd	Pr	Pt	Rb	Re	Rh	Ru	S	Sb	Sc
1.22	2.0.E-04	3.8.E-01	1.4.E-03	6.4.E-04	9.7.E-05	5.2.E-05	7.0.E-02	7.4.E-03	5.4.E-05	2.7.E-04	4.4.E+04	1.1.E-03	8.2.E-03
4.34	7.7.E-05	3.6.E-01	6.9.E-04	1.8.E-04	3.7.E-05	1.3.E-05	1.8.E-02	2.2.E-03	1.6.E-05	1.3.E-04	9.2.E+03	6.7.E-04	1.0.E-03
9	5.4.E-05	3.8.E-01	4.1.E-04	4.5.E-05	1.4.E-05	6.1.E-06	5.9.E-03	5.1.E-04	3.4.E-06	3.4.E-05	1.7.E+03	4.2.E-04	2.7.E-04
36.5	8.6.E-06	1.6.E+00	2.0.E-04	1.7.E-06	5.4.E-06	1.7.E-06	1.5.E-03	2.6.E-05	4.5.E-07	4.9.E-06	9.4.E+01	6.7.E-04	7.3.E-05
69	4.5.E-06	1.5.E+00	1.3.E-04	6.5.E-07	1.5.E-06	8.7.E-07	9.5.E-04	1.9.E-05	2.0.E-07	8.8.E-07	4.2.E+01	1.8.E-04	3.2.E-05
106	4.5.E-06	1.4.E+00	1.8.E-04	3.9.E-06	1.4.E-06	3.8.E-07	7.8.E-04	1.3.E-05	4.0.E-07	1.5.E-05	3.1.E+01	1.2.E-04	1.1.E-05
139	3.3.E-06	1.2.E+00	1.2.E-04	2.8.E-06	2.1.E-06	2.2.E-07	6.7.E-04	1.1.E-05	1.8.E-07	2.8.E-06	2.8.E+01	7.0.E-05	2.2.E-05
195	1.9.E-06	5.0.E-01	1.0.E-04	7.9.E-08	5.7.E-07	3.0.E-07	5.5.E-04	7.5.E-06	1.9.E-07	4.0.E-06	2.5.E+01	7.4.E-05	1.5.E-05
1093	4.0.E-07	2.0.E-01	8.7.E-05	0.0.E+00	1.8.E-07	1.0.E-07	3.0.E-04	2.7.E-06	1.7.E-07	0.0.E+00	5.9.E+00	3.2.E-05	1.0.E-05
21779	1.2.E-06	1.3.E-01	1.7.E-04	2.4.E-06	3.9.E-07	9.9.E-10	1.4.E-03	1.9.E-07	1.5.E-07	3.0.E-06	9.4.E-01	2.7.E-05	6.7.E-06
Estim. Unc. (%)	NA	10-50	50	NA	NA	NA	NA	NA	NA	NA	10	NA	NA

Time (min.)	Se	Si	Sm	Sn	Sr	Ta	Tb	Te	Th	Ti	Tl	Tm	U
1.22	8.6.E-01	2.9.E+02	1.1.E-04	3.5.E-03	1.4.E+01	2.5.E-05	2.1.E-05	2.7.E-05	1.2.E-05	5.0.E-02	4.9.E-05	5.7.E-06	1.1.E-04
4.34	3.8.E-01	2.4.E+02	4.2.E-05	2.3.E-03	3.5.E+00	2.5.E-05	6.6.E-06	2.8.E-05	1.6.E-05	2.2.E-01	1.2.E-05	4.1.E-06	6.4.E-05
9	3.2.E-01	2.3.E+02	1.8.E-05	1.6.E-03	7.9.E-01	3.1.E-06	3.0.E-06	1.2.E-04	7.0.E-06	9.9.E-02	4.7.E-06	1.4.E-06	2.7.E-05
36.5	2.1.E-01	2.2.E+02	5.2.E-06	2.3.E-03	1.1.E-01	6.8.E-07	1.0.E-06	2.1.E-04	2.5.E-06	1.9.E-02	9.8.E-07	3.7.E-07	1.5.E-05
69	7.5.E-02	1.7.E+02	1.2.E-06	1.1.E-03	8.4.E-02	2.5.E-06	3.9.E-07	1.9.E-04	2.4.E-07	6.2.E-03	9.7.E-07	1.3.E-07	1.0.E-05
106	3.6.E-02	1.4.E+02	2.1.E-06	1.1.E-03	7.6.E-02	2.8.E-08	2.2.E-07	1.6.E-04	3.1.E-07	3.8.E-03	1.0.E-06	8.0.E-08	8.9.E-06
139	3.3.E-02	1.2.E+02	2.1.E-06	1.0.E-03	6.7.E-02	4.2.E-06	2.3.E-07	1.5.E-04	1.3.E-06	4.0.E-03	6.7.E-07	3.4.E-07	7.7.E-06
195	2.2.E-02	9.7.E+01	7.8.E-07	4.4.E-04	5.4.E-02	5.5.E-06	1.4.E-08	9.7.E-05	1.5.E-07	2.4.E-03	6.4.E-07	5.2.E-08	4.3.E-06
1093	4.2.E-03	7.1.E+01	2.2.E-07	1.3.E-04	1.8.E-02	4.4.E-06	0.0.E+00	2.2.E-05	1.0.E-07	8.9.E-04	1.7.E-07	1.9.E-08	9.5.E-07
21779	0.0.E+00	1.1.E+01	2.5.E-07	6.1.E-04	6.5.E-03	3.9.E-06	3.5.E-08	1.9.E-06	1.6.E-07	8.8.E-04	1.0.E-06	0.0.E+00	6.4.E-07
Estim. Unc. (%)	NA	10	NA	50	10-50	NA	NA	NA	NA	10-50	NA	NA	50

Time (min.)	W	V	Y	Yb	Zn	Zr
1.22	3.4.E-04	1.9.E-02	1.6.E-03	3.5.E-05	2.8.E+00	1.8.E-03
4.34	4.8.E-04	3.2.E-02	4.0.E-04	1.7.E-05	8.3.E-01	2.4.E-03
9	4.6.E-04	6.6.E-02	1.4.E-04	9.0.E-06	2.0.E-01	1.0.E-03
36.5	1.3.E-04	5.1.E-01	4.1.E-05	2.6.E-06	1.0.E-01	1.6.E-04
69	9.3.E-05	3.5.E-01	1.5.E-05	6.3.E-07	3.3.E-02	9.8.E-05
106	7.0.E-05	2.1.E-01	1.4.E-05	7.4.E-07	6.4.E-02	6.9.E-05
139	5.0.E-05	1.6.E-01	1.4.E-05	2.6.E-07	2.2.E-02	5.1.E-05
195	4.5.E-05	1.1.E-01	2.8.E-06	2.3.E-07	2.7.E-02	2.2.E-05
1093	1.8.E-05	4.3.E-02	8.9.E-07	4.9.E-07	1.3.E-02	6.9.E-06
21779	5.0.E-06	3.1.E-03	2.3.E-06	1.4.E-07	1.3.E-01	2.8.E-05
Estim. Unc. (%)	NA	10-50	NA	NA	10-50	NA

Calculated Si release rate according to Gislason and Oelkers, 2003

Time (min.)	r+ (BET)
1.2	7.8.E+00
4.3	8.7.E+00
9	5.0.E+00
36.5	2.0.E+01
69	1.7.E+01
106	1.7.E+01
139	1.7.E+01
195	1.8.E+01
1093	1.6.E+01
21779	9.5.E+00